Ziv-Zakai Bound for DOAs Estimation

Zongyu Zhang, *Student Member, IEEE,* Zhiguo Shi, *Senior Member, IEEE,* and Yujie Gu, *Senior Member, IEEE*

***Abstract*—Lower bounds on the mean square error (MSE) play an important role in evaluating the estimation performance of nonlinear parameters including direction-of-arrival (DOA). Among numerous known bounds, the well-accepted Cramér-Rao bound (CRB) lower bounds the MSE in the asymptotic region only, due to its locality. By contrast, the less-adopted Ziv-Zakai bound (ZZB) is restricted by the single source assumption, although it is global tight. In this paper, we first derive an explicit ZZB applicable for hybrid coherent/incoherent multiple sources DOA estimation. In detail, we incorporate Woodbury matrix identity and Sylvester's determinant theorem to generalize the ZZB from single source DOA estimation to multiple sources DOA estimation, which, unfortunately, becomes invalid when it is far away from the asymptotic region. We then introduce the order statistics to describe the effect of ordering process during MSE calculation on the change of *a priori* distribution of DOAs, such that the derived ZZB can keep a tight bound on the MSE outside the asymptotic region. The derived ZZB is for the first time formulated as the function of the coherent coefficients between the coherent sources, and reveals the relationship between the MSE convergency in the *a priori* performance region and the number of sources. Moreover, the derived ZZB also provides a unified tight bound for both overdetermined DOAs estimation and underdetermined DOAs estimation. Simulation results demonstrate the obvious advantages of the derived ZZB over the CRB on evaluating and predicting the estimation performance of multiple sources DOA.**

***Index Terms*—Coherence, Cramér-Rao bound, directions-of-arrival estimation, mean square error, order statistics, permutation ambiguity, Ziv-Zakai bound.**

I. Introduction

DIRECTION-of-arrival (DOA) estimation is a fundamental problem in many array processing applications including radar, sonar, navigation, and wireless communications [1]. In the past decades, multiple sources DOA estimation has attracted great research interest, the majority of which concentrated on the algorithm design. Among them, the typical ones include multiple signal classification (MUSIC) [2–4], estimation of signal parameters via rotational invariant techniques (ESPRIT) [5–7], sparsity-based algorithms [8–10], and machine learning based algorithms [11–13].

Mean square error (MSE) is commonly used to evaluate the performance of estimators. However, as a typical nonlinear parameter estimation problem, there is no exact closed-form minimum MSE solution for DOAs estimation, which motivates to find MSE lower bounds (see, for example, [14] and the references therein). Among them, Cramér-Rao bound (CRB) [15] is the most widely used one due to its easy evaluation in general. The closed-form expression of CRB for DOAs estimation is given in [16, 17] as the inverse of Fisher information matrix. To overcome the singularity of Fisher information matrix in the underdetermined condition, coarray CRB is given in [18, 19] by deriving the nonsingular Fisher information matrix for coarray-based DOAs estimation. These CRBs treat the DOAs as unknown deterministic, and lower bound the MSE in estimating any specific value of the parameter. This property limits CRB in utilizing the *a priori* information about the parameter space, and correspondingly, CRB is only tight in the asymptotic region. In order to overcome the locality of the classical CRB, numerous Bayesian bounds have been proposed in the past few decades [14], among which the typical one is covariance inequality-based bounds [20] like Bayesian CRB (BCRB) [1], Weiss-Weinstein bound (WWB) [21], Reuven-Messer bound (RMB) [22], Bayesian Abel bound (RAB) [23] and Bobrovsky-Zakai bound (BZB) [24]. Although aforementioned bounds can potentially provide tighter bound, they do rely on higher order derivative, optimization over free variables and empirical testing point selection [14].

As another typical Bayesian bound, Ziv-Zakai bound (ZZB) enables to provide a global tight bound on the MSE over a wide range of signal-to-noise ratio (SNR). ZZB is originally proposed in [25] (with improvement in [26, 27]) by considering a scalar estimation problem, where the time delay is assumed to follow a uniform *a priori* distribution. Since then, the ZZBs for specific scalar parameter estimation problems have been widely studied [28–35], e.g., single source DOA estimation exploiting linear arrays [28, 30]. On the other hand, a unified expression of ZZB for vector parameter estimation with arbitrary *a priori* distribution is first derived in [36], which provides a promising framework for the derivation of ZZB on DOA vector estimation. However, it remains challenges in deriving an explicit ZZB due to the involved high dimensional integration and constrained optimization. Although an explicit ZZB for two-dimensional DOA estimation is derived in [37], the involved Sherman-Morrison formula and matrix determinant lemma make it only appropriate for single source case. Furthermore, its uniform distribution assumption on $\sin\theta$ rather than on the DOA θ itself, is impractical for DOA estimation, because it implies that, the source signal impinges on the array from boresight with the highest probability, and the probability gradually decreases with the DOA deviating from the boresight. Hence, the existing ZZBs for single source DOA estimation are difficult to be extended to multiple sources scenario, where the main challenges are:

- With the number of sources increasing, the numerical

Z. Zhang is supported by the China Scholarship Council for his stay at the University of Pisa. The work of Z. Zhang and Z. Shi is supported in part by National Natural Science Foundation of China (No. U21A20456, 61901413, 61772467). (Corresponding authors: Zhiguo Shi and Yujie Gu).

Z. Zhang is with the College of Information Science and Electronic Engineering, Zhejiang University, Hangzhou 310027, China, and also with the Department of Information Engineering, University of Pisa, Pisa, PI 56122, Italy (email: zongyu_zhang@zju.edu.cn).

Z. Shi is with the College of Information Science and Electronic Engineering, Zhejiang University, Hangzhou 310027, China (email: shizg@zju.edu.cn).

Y. Gu is with Advanced Safety & User Experience, Aptiv, Agoura Hills, CA 91301, USA (email: guyujie@hotmail.com).

Welcome to contact the authors to acquire ZZB MATLAB simulation demo.

solution suffer from heavier computational burden, such that an explicit ZZB solution is required. Meanwhile, the existing explicit ZZB derived from Sherman-Morrison formula and matrix determinant lemma is appropriate for single source DOA estimation only.

- For multiple sources DOA estimation, there naturally exists permutation ambiguity during MSE calculation. However, the ordering process for the elimination of permutation ambiguity implicitly changes the *a priori* distribution of DOAs and affects the MSE of DOAs estimation outside the asymptotic region, which makes ZZB derived from the existing framework still invalid in the *a priori* performance region.
- For multiple sources DOA estimation, the mutual coherence among coherent sources is generally unavoidable due to multipath propagation (see, [38–40] and the references therein), whose effect on the ZZB is still unclear.

Facing these challenges, in this paper, we consider the derivation of ZZB for a hybrid coherent/incoherent multiple sources DOA estimation. By utilizing Woodbury matrix identity and Sylvester's determinant theorem, we first follow the derivation in [37] to generalize the ZZB for single source DOA estimation to multiple sources DOA estimation. However, such straightforward generalization does not consider the permutation ambiguity arising in MSE calculation for multiple sources DOA estimation, which makes such a generalized ZZB still invalid in the *a priori* performance region. To this end, we for the first time introduce the order statistics to describe the effect of the permutation ambiguity elimination on the ZZB, such that the derived ZZB keeps tight for the evaluation of DOA estimators outside the asymptotic region. The derived ZZB for DOAs estimation is formulated as an explicit function of the number of sources, the number of array sensors, the number of snapshots, the *a priori* distribution and SNRs of sources, array observation data, and the coherent coefficient. Further more, the derived ZZB provides a unified expression for both overdetermined DOAs estimation and underdetermined DOAs estimation, and also explicitly reveals the MSE convergence performance in the *a priori* performance region with respect to (w.r.t.) the number of sources. Simulations demonstrate the effectiveness of the derived ZZB to predict multiple sources DOA estimation performance, benefited from its obvious threshold effect. Compared with the widely used CRB, the derived ZZB provides a tight bound over a wider range of SNR, and clearly reveals the MSE convergence performance in the *a priori* performance region and the effect of the coherent coefficient in the transition region.

The rest of this paper is organized as follows. We introduce a hybrid multiple sources model, MSE and CRB in Section II, and the related ZZB preliminaries in Section III. Then, in Section IV we derive a ZZB as an explicit function of multiple sources, where permutation ambiguity in DOAs estimation is also considered. Simulations are performed to demonstrate the advantages of the derived ZZB in Section V. Finally, we make our conclusions in Section VI.

II. Signal Model, MSE and CRB

Assuming K far-field narrowband signals impinging on a linear array consisting of M sensors located at $\{d_1, d_2, \cdots, d_M\}$ from directions $\boldsymbol{\theta} = [\theta_1, \theta_2, \cdots, \theta_K]^{\mathrm{T}}$, where, without loss of generality, the first L $(1 \leq L \leq K)$ sources are assumed to be mutually coherent, while the left $K-L$ sources are incoherent with each other and independent with the first L signals. Here, $[\,\cdot\,]^{\mathrm{T}}$ denotes the transpose. The array observation data are modeled as

$$\begin{aligned}\boldsymbol{x}(t) &= \sum_{k=1}^{L} \boldsymbol{a}(\theta_k)\beta_k s_1(t) + \sum_{k=L+1}^{K} \boldsymbol{a}(\theta_k) s_k(t) + \boldsymbol{n}(t) \\ &= \boldsymbol{A}(\boldsymbol{\theta})\boldsymbol{s}(t) + \boldsymbol{n}(t), \forall t = 1, 2, \cdots, T,\end{aligned} \tag{1}$$

where $\boldsymbol{A}(\boldsymbol{\theta}) = [\boldsymbol{a}(\theta_1), \boldsymbol{a}(\theta_2), \cdots, \boldsymbol{a}(\theta_K)] \in \mathbb{C}^{M\times K}$ is the steering matrix with the k-th column

$$\boldsymbol{a}(\theta_k) = \left[e^{-j\frac{2\pi}{\lambda}d_1 \sin\theta_k}, \cdots, e^{-j\frac{2\pi}{\lambda}d_M \sin\theta_k}\right]^{\mathrm{T}} \tag{2}$$

denoting the steering vector of the k-th source with λ representing the wavelength, $\boldsymbol{s}(t) = [\boldsymbol{\beta}^{\mathrm{T}} s_1(t), s_{L+1}(t), \cdots, s_K(t)]^{\mathrm{T}} \in \mathbb{C}^K$ denotes the K signals with $\boldsymbol{\beta} = [\beta_1, \cdots, \beta_L]^{\mathrm{T}} \in \mathbb{C}^L$ containing the coherent coefficient β_l between the l-th $(1 \leq l \leq L)$ coherent signal $\beta_l s_1(t)$ and the reference signal $s_1(t)$ (i.e., $\beta_1 = 1$), and $\boldsymbol{n}(t) \sim \mathcal{CN}(\boldsymbol{0}_M, \sigma_n^2 \boldsymbol{I}_M)$ is the zero-mean additive white Gaussian noise independent of the signals with $\boldsymbol{0}_M$, σ_n^2, and $\boldsymbol{I}_M$ respectively denoting an M-dimensional all-zero vector, the noise power, and an M-dimensional identity matrix. Here, T denotes the number of snapshots.

Without loss of generality, we make the following assumptions:

Assumption 1. *All the incoherent signals $s_k(t), k = 1, L+1, \cdots, K$ are sampled from zero-mean, stationary complex Gaussian stochastic processes.*

Assumption 2. *The DOAs of the signals are distinct (say, $\theta_\imath \neq \theta_\jmath$ $\forall \imath \neq \jmath$).*

Assumption 3. *Each DOA follows the same uniform distribution $\theta_k \sim \mathcal{U}[\vartheta_{\min}, \vartheta_{\max}], \forall k = 1, 2, \cdots, K$.*

Thus, the theoretical covariance matrix of $\boldsymbol{x}(t)$ given $\boldsymbol{\theta}$ is

$$\boldsymbol{R}_{\boldsymbol{x}|\boldsymbol{\theta}} = \mathbb{E}\{\boldsymbol{x}(t)\boldsymbol{x}^{\mathrm{H}}(t)\} = \boldsymbol{A}(\boldsymbol{\theta})\boldsymbol{\Sigma}\boldsymbol{A}^{\mathrm{H}}(\boldsymbol{\theta}) + \sigma_n^2 \boldsymbol{I}_M, \tag{3}$$

where

$$\boldsymbol{\Sigma} = \mathbb{E}\left\{\boldsymbol{s}(t)\boldsymbol{s}^{\mathrm{H}}(t)\right\} = \text{block diag}[\boldsymbol{\Sigma}_{co}, \boldsymbol{\Sigma}_{in}] \tag{4}$$

with

$$\boldsymbol{\Sigma}_{co} = \boldsymbol{\beta}\boldsymbol{\beta}^{\mathrm{H}}\sigma_1^2 \tag{5}$$

denoting the covariance matrix corresponding to the first L coherent signals, and

$$\boldsymbol{\Sigma}_{in} = \text{diag}\left[\sigma_{L+1}^2, \cdots, \sigma_K^2\right] \tag{6}$$

denoting the power of the left $K-L$ incoherent signals. Here, $\mathbb{E}\{\,\cdot\,\}$ denotes the statistical expectation, $[\,\cdot\,]^{\mathrm{H}}$ represents the Hermitian transpose, $\text{block diag}[\,\cdot\,]$ and $\text{diag}[\,\cdot\,]$ respectively denote the block diagonal matrix and the diagonal matrix, and σ_k^2 $(k = 1, \cdots, K)$ denotes the power of the k-th source.

Similar to other parameter estimation problems, the MSE defined as

$$\text{MSE} = \frac{1}{K}\sum_{k=1}^{K}\mathbb{E}\left\{\left(\hat{\theta}_k - \theta_k\right)^2\right\} = \frac{1}{K}\text{Tr}\{\boldsymbol{R}_{\boldsymbol{\epsilon}}\} \tag{7}$$

is a well accepted metric to evaluate the estimation accuracy of DOA estimators, where $\hat{\theta}_k$ is the estimate of θ_k, and

$$\boldsymbol{R}_{\boldsymbol{\epsilon}} = \mathbb{E}\left\{\boldsymbol{\epsilon}\boldsymbol{\epsilon}^{\mathrm{T}}\right\} = \mathbb{E}\left\{(\hat{\boldsymbol{\theta}}-\boldsymbol{\theta})(\hat{\boldsymbol{\theta}}-\boldsymbol{\theta})^{\mathrm{T}}\right\} \tag{8}$$

is the error correlation matrix. Here, $\mathrm{Tr}\{\cdot\}$ denotes the trace of a matrix. It is worth noting that, the definition of MSE for DOA estimation implies the following assumption:

Assumption 4. *All DOAs make the same contribution for MSE calculation, namely, they have an equal weight.*

As a widely used lower bound in evaluating the variance of DOA estimators, CRB is the inverse of the Fisher information, where the $\imath\jmath$-th entry of the Fisher information matrix $\boldsymbol{J}$ w.r.t. $\boldsymbol{\theta}$ is given by [1]

$$\boldsymbol{J}_{\imath\jmath} = T\mathrm{Tr}\left\{\frac{\partial \boldsymbol{R}_{\boldsymbol{x}|\boldsymbol{\theta}}}{\partial\theta_\imath}\boldsymbol{R}_{\boldsymbol{x}|\boldsymbol{\theta}}^{-1}\frac{\partial \boldsymbol{R}_{\boldsymbol{x}|\boldsymbol{\theta}}}{\partial\theta_\jmath}\boldsymbol{R}_{\boldsymbol{x}|\boldsymbol{\theta}}^{-1}\right\}. \tag{9}$$

It is observed that, due to the uniform distribution, there is no *a priori* information of $\boldsymbol{\theta}$ contributing to Fisher information even if in Bayesian CRB (BCRB) [1], which makes CRB only tight in the asymptotic region.

III. ZZB Preliminaries

The extended ZZB for vector parameter estimation given in [36, Eq. (32)] to lower bound the error correlation matrix is[1]

$$\begin{aligned}&\boldsymbol{w}^{\mathrm{T}}\boldsymbol{R}_{\boldsymbol{\epsilon}}\boldsymbol{w}\\ &\geq \frac{1}{2}\int_0^\infty \max_{\boldsymbol{\delta}:\boldsymbol{w}^{\mathrm{T}}\boldsymbol{\delta}=h}\left[\int_{\mathbb{R}^K}(f_{\boldsymbol{\theta}}(\boldsymbol{\varphi})+f_{\boldsymbol{\theta}}(\boldsymbol{\varphi}+\boldsymbol{\delta}))P_{\min}(\boldsymbol{\varphi},\boldsymbol{\varphi}+\boldsymbol{\delta})d\boldsymbol{\varphi}\right]hdh,\end{aligned} \tag{10}$$

where $\boldsymbol{w}\in\mathbb{R}^K$ represents a normalized weight vector (i.e., the ℓ_2 norm $\|\boldsymbol{w}\|_2 = 1$), $f_{\boldsymbol{\theta}}(\boldsymbol{\varphi}) \triangleq f(\boldsymbol{\theta})|_{\boldsymbol{\theta}=\boldsymbol{\varphi}}$ with $f(\boldsymbol{\theta})$ denoting the *a priori* probability density function (PDF) of $\boldsymbol{\theta}$, and $P_{\min}(\boldsymbol{\varphi},\boldsymbol{\varphi}+\boldsymbol{\delta})$ is the minimum probability of error of the binary hypothesis testing problem

$$\begin{aligned}&\mathcal{H}_0: \boldsymbol{\theta}=\boldsymbol{\varphi}; \qquad \boldsymbol{x}\sim f(\boldsymbol{x}|\boldsymbol{\varphi})\\ &\mathcal{H}_1: \boldsymbol{\theta}=\boldsymbol{\varphi}+\boldsymbol{\delta}; \quad \boldsymbol{x}\sim f(\boldsymbol{x}|\boldsymbol{\varphi}+\boldsymbol{\delta})\end{aligned} \tag{11}$$

with

$$\begin{aligned}\Pr(\mathcal{H}_0) &= \frac{f_{\boldsymbol{\theta}}(\boldsymbol{\varphi})}{f_{\boldsymbol{\theta}}(\boldsymbol{\varphi})+f_{\boldsymbol{\theta}}(\boldsymbol{\varphi}+\boldsymbol{\delta})}\\ \Pr(\mathcal{H}_1) &= 1-\Pr(\mathcal{H}_0).\end{aligned} \tag{12}$$

Here, $f(\boldsymbol{x}|\boldsymbol{\varphi})$ and $f(\boldsymbol{x}|\boldsymbol{\varphi}+\boldsymbol{\delta})$ are respectively the conditional PDFs of $\boldsymbol{x}$ given $\boldsymbol{\theta}=\boldsymbol{\varphi}$ and $\boldsymbol{\theta}=\boldsymbol{\varphi}+\boldsymbol{\delta}$, and $\Pr(\cdot)$ denotes probability. With Assumption 4, the weight vector $\boldsymbol{w}$ in DOAs estimation becomes

$$\boldsymbol{w} = \frac{1}{\sqrt{K}}\mathbf{1}_K, \tag{13}$$

where $\mathbf{1}_K$ denotes a K-dimensional all-one vector. Thus, (10) can be written as

$$\begin{aligned}\frac{1}{K}\mathbf{1}_K^{\mathrm{T}}\boldsymbol{R}_{\boldsymbol{\epsilon}}\mathbf{1}_K \geq \frac{1}{2}\int_0^\infty \max_{\boldsymbol{\delta}:\mathbf{1}_K^{\mathrm{T}}\boldsymbol{\delta}=\sqrt{K}h}&\left[\int_{\mathbb{R}^K}(f_{\boldsymbol{\theta}}(\boldsymbol{\varphi})+f_{\boldsymbol{\theta}}(\boldsymbol{\varphi}+\boldsymbol{\delta}))\right.\\ &\left.\times P_{\min}(\boldsymbol{\varphi},\boldsymbol{\varphi}+\boldsymbol{\delta})d\boldsymbol{\varphi}\right]hdh.\end{aligned} \tag{14}$$

[1]The valley filling operation in [36, Eq. (32)] is ignored since it is proved in [37] that the valley filling operation does not have an effect in DOA estimation context.

For single source case (i.e., $K=1$), the vector $\boldsymbol{\theta}$ degrades to a scalar θ, $\delta = h$, and (14) becomes

$$\begin{aligned}&\mathbb{E}\left\{\left(\hat{\theta}-\theta\right)^2\right\}\\ &\geq \frac{1}{2}\int_0^\infty\int_{-\infty}^{+\infty}(f_\theta(\varphi)+f_\theta(\varphi+h))\,P_{\min}(\varphi,\varphi+h)d\varphi hdh,\end{aligned} \tag{15}$$

which also has been investigated in the ZZB for scalar parameter estimation [30]. On the contrary, for multiple sources case (i.e., $K\geq 2$), it's still challenging for ZZB to evaluate the performance of DOA estimators straightforwardly due to K-dimensional integration and optimization in (14).

IV. Derivation of ZZB for DOAs Estimation

In this section, we derive a ZZB for DOAs estimation in an explicit way, where the number of sources, the number of array sensors, the number of snapshots, the *a priori* distribution and SNRs of sources, array observation data, and the coherent coefficient are served as explicit factors. In subsection IV-A, we follow the derivation framework in [37] to generalize the ZZB for single source DOA estimation to multiple sources DOA estimation, which, however, is still invalid for lower bounding the MSE performance outside the asymptotic region. Then, considering the permutation ambiguity arising in MSE calculation for multiple sources DOA estimation, in subsection IV-B, we introduce the order statistics to make the derived ZZB global tight in evaluating the MSE for multiple sources DOA estimation.

A. Generalized ZZB for Multiple Sources Case

It is worth noting that, the utilization of Sherman-Morrison formula and matrix determinant lemma in [37] makes it appropriate for single source case only, which, accordingly, hinders the ZZB derivation in multiple sources scenario. Instead, for the hybrid coherent/incoherent multiple sources considered in this paper, we introduce Woodbury matrix identity and Sylvester's determinant theorem to generalize the ZZB as an explicit function of multiple sources.

For the array observation data matrix $\boldsymbol{X} = [\boldsymbol{x}(1),\cdots,\boldsymbol{x}(T)] \in \mathbb{C}^{M\times T}$, $P_{\min}(\boldsymbol{\varphi},\boldsymbol{\varphi}+\boldsymbol{\delta})$ is lower bounded as [41, p. 79]

$$\begin{aligned}&P_{\min}(\boldsymbol{\varphi},\boldsymbol{\varphi}+\boldsymbol{\delta})\\ &\geq e^{\left[\mu(p;\boldsymbol{\delta})+\frac{1}{8}\frac{\partial^2\mu(p;\boldsymbol{\delta})}{\partial p^2}\right]}\mathcal{Q}\left(\frac{1}{2}\sqrt{\frac{\partial^2\mu(p;\boldsymbol{\delta})}{\partial p^2}}\right)\Bigg|_{p=\frac{1}{2}}\\ &\triangleq P(\boldsymbol{\delta}),\end{aligned} \tag{16}$$

where

$$\mathcal{Q}(z) = \int_z^\infty \frac{1}{\sqrt{2\pi}}e^{-\frac{v^2}{2}}dv \tag{17}$$

is the tail distribution function of the standard normal distribution, and

$$\mu(p;\boldsymbol{\delta}) = \ln\int f(\boldsymbol{X}|\boldsymbol{\varphi}+\boldsymbol{\delta})^p f(\boldsymbol{X}|\boldsymbol{\varphi})^{1-p}d\boldsymbol{X} \tag{18}$$

is the semi-invariant moment generating function. According to Appendix A, $\mu(p;\boldsymbol{\delta})|_{p=\frac{1}{2}}$ and $\frac{\partial^2\mu(p;\boldsymbol{\delta})}{\partial p^2}\big|_{p=\frac{1}{2}}$ in (16) are approximated as

$$\mu(p;\boldsymbol{\delta})|_{p=\frac{1}{2}} \approx \begin{cases} -\frac{1}{8}\boldsymbol{\delta}^{\mathrm{T}}\boldsymbol{J}\boldsymbol{\delta}, & \boldsymbol{\delta}\in\Delta \\ T\left[\ln\frac{4(1+M\eta_1\|\boldsymbol{\beta}\|_2^2)}{(2+M\eta_1\|\boldsymbol{\beta}\|_2^2)^2}+\sum\limits_{k=L+1}^{K}\ln\frac{4(1+M\eta_k)}{(2+M\eta_k)^2}\right], & \boldsymbol{\delta}\notin\Delta \end{cases}, \tag{19}$$

and

$$\left.\frac{\partial^2\mu(p;\boldsymbol{\delta})}{\partial p^2}\right|_{p=\frac{1}{2}} \approx \begin{cases} \boldsymbol{\delta}^{\mathrm{T}}\boldsymbol{J}\boldsymbol{\delta}, & \boldsymbol{\delta}\in\Delta \\ 8T\left[\left(\frac{M\eta_1\|\boldsymbol{\beta}\|_2^2}{2+M\eta_1\|\boldsymbol{\beta}\|_2^2}\right)^2+\sum\limits_{k=L+1}^{K}\left(\frac{M\eta_k}{2+M\eta_k}\right)^2\right], & \boldsymbol{\delta}\notin\Delta \end{cases}, \tag{20}$$

where $\eta_k = \frac{\sigma_k^2}{\sigma_n^2}$ denotes the SNR of the k-th source, and Δ denotes the region

$$\Delta=\left\{\boldsymbol{\delta}\colon \boldsymbol{\delta}^{\mathrm{T}}\boldsymbol{J}\boldsymbol{\delta}\leq 8T\left[\left(\frac{M\eta_1\|\boldsymbol{\beta}\|_2^2}{2+M\eta_1\|\boldsymbol{\beta}\|_2^2}\right)^2+\sum_{k=L+1}^{K}\left(\frac{M\eta_k}{2+M\eta_k}\right)^2\right]\right\}. \tag{21}$$

Accordingly, $P(\boldsymbol{\delta})$ in (16) is approximated as

$$P(\boldsymbol{\delta}) \approx \begin{cases} P_{\mathrm{S}}(\boldsymbol{\delta}), & \boldsymbol{\delta}\in\Delta \\ P_{\mathrm{L}}, & \boldsymbol{\delta}\notin\Delta \end{cases} \tag{22}$$

with

$$P_{\mathrm{S}}(\boldsymbol{\delta}) = \mathcal{Q}\left(\frac{1}{2}\sqrt{\boldsymbol{\delta}^{\mathrm{T}}\boldsymbol{J}\boldsymbol{\delta}}\right), \tag{23}$$

and P_{L} (24) is shown at the bottom of this page.

It should be pointed out that, the $P_{\mathrm{S}}(\boldsymbol{\delta})$ derived here is appropriate for multiple sources case although it has the same expression as [37, Eq. (D. 13)]. To be more specific, the determinants of $\mu(p;\boldsymbol{\delta})|_{p=\frac{1}{2}}$ in [37] are calculated using matrix determinant lemma in [37, Eq. (B. 16)] and [37, Eq. (B. 17)], from which the $P_{\mathrm{S}}(\boldsymbol{\delta})$ is finally derived. Considering the fact that the use of matrix determinant lemma in [37] implied the single source assumption, the $P_{\mathrm{S}}(\boldsymbol{\delta})$ derived there is naturally restricted by single source case. On the contrary, we perform the Taylor expansion directly on the $\mu(p;\boldsymbol{\delta})|_{p=\frac{1}{2}}$ and $\left.\frac{\partial^2\mu(p;\boldsymbol{\delta})}{\partial p^2}\right|_{p=\frac{1}{2}}$ that preserve the matrix determinants to derive the $P_{\mathrm{S}}(\boldsymbol{\delta})$, during which the assumption about number of sources has not been involved. Therefore, the $P_{\mathrm{S}}(\boldsymbol{\delta})$ is appropriate for both single source and multiple sources simultaneously. Besides, we adopt Woodbury matrix identity and Sylvester's determinant theorem rather than Sherman-Morrison formula and matrix determinant lemma in [37] to derive P_{L}, which, not only makes the P_{L} work for multiple sources, but enables us for the first time to formulate it as an explicit function of coherent coefficients $\boldsymbol{\beta}$. Moreover, the derived P_{L} is also a function of the number of sources, which is approximately[2] same as that in [37] when $K=1$.

Since K DOAs are independent, the K-dimensional integration in (14) becomes

$$\begin{aligned} &\int_{\mathbb{R}^K}\left(f_{\boldsymbol{\theta}}(\boldsymbol{\varphi})+f_{\boldsymbol{\theta}}(\boldsymbol{\varphi}+\boldsymbol{\delta})\right)P_{\min}(\boldsymbol{\varphi},\boldsymbol{\varphi}+\boldsymbol{\delta})d\boldsymbol{\varphi} \\ &\geq \frac{2P(\boldsymbol{\delta})}{\zeta^K}\int_{\Phi}d\boldsymbol{\varphi} \\ &= 2P(\boldsymbol{\delta})\frac{\prod_{k=1}^{K}(\zeta-|\delta_k|)}{\zeta^K}, \end{aligned} \tag{25}$$

where

$$\Phi = \{\boldsymbol{\varphi}|\varphi_k\in[\vartheta_{\min},\vartheta_{\max}-|\delta_k|], k=1,2,\cdots,K\} \tag{26}$$

is the K-dimensional integration region, $\zeta=\vartheta_{\max}-\vartheta_{\min}$ denotes the range of DOAs, and $|\delta_k|$ is the absolute value of the k-th element in $\boldsymbol{\delta}$.

According to the derivation in Appendix B, the ZZB for DOAs estimation is generalized for multiple sources as

$$\frac{1}{K}\mathbf{1}_K^{\mathrm{T}}\boldsymbol{R}_{\boldsymbol{\epsilon}}\mathbf{1}_K \geq \frac{12P_{\mathrm{L}}\mathrm{Tr}\{\boldsymbol{R}_{\boldsymbol{\theta}}\}}{(K+1)(K+2)}+\Gamma_{\frac{3}{2}}(\tilde{u})\,\frac{\mathbf{1}_K^{\mathrm{T}}\boldsymbol{J}^{-1}\mathbf{1}_K}{K}, \tag{27}$$

where

$$\boldsymbol{R}_{\boldsymbol{\theta}} = \frac{\zeta^2}{12}\boldsymbol{I}_K \tag{28}$$

is the *a priori* covariance matrix of $\boldsymbol{\theta}$, $\Gamma_{\frac{3}{2}}(\cdot)$ is the normalized incomplete Gamma function

$$\Gamma_g(q) = \frac{1}{\Gamma(g)}\int_0^q e^{-\xi}\xi^{g-1}d\xi \tag{29}$$

with $\Gamma(\frac{3}{2})=\frac{\sqrt{\pi}}{2}$ being the Gamma function, and

$$\tilde{u} = \frac{K\tilde{h}^2}{8\mathbf{1}_K^{\mathrm{T}}\boldsymbol{J}^{-1}\mathbf{1}_K} \tag{30}$$

with $\tilde{h}$ (31) shown at the bottom of this page. Obviously, the generalized ZZB in (27) lower bounds the error correlation matrix, one special case of which is the MSE we sought. Specifically, considering that the MSE defined in (7) is only related to the diagonal elements in error correlation matrix $\boldsymbol{R}_{\boldsymbol{\epsilon}}$ (also, the diagonal elements in $\boldsymbol{J}^{-1}$ [42]), the MSE of DOAs estimation can be lower bounded by the generalized ZZB as

$$\mathrm{MSE} \geq \frac{12P_{\mathrm{L}}\mathrm{Tr}\{\boldsymbol{R}_{\boldsymbol{\theta}}\}}{(K+1)(K+2)}+\Gamma_{\frac{3}{2}}(\tilde{u})\,\frac{\mathrm{Tr}\{\boldsymbol{J}^{-1}\}}{K}. \tag{32}$$

It can be observed from (32) that only the first term is a function of the *a priori* distribution of $\boldsymbol{\theta}$ via $\boldsymbol{R}_{\boldsymbol{\theta}}$, while the second term indicates that the ZZB converges to the CRB in the asymptotic region.

[2]Our derivation of P_{L} is consistent with [37, Eq. (C. 13)]. However, an extra approximation was made in [37, Eq. (C. 13)]. Hence, we mention "approximately" here.

$$P_{\mathrm{L}}=e^{T\left[\ln\frac{4(1+M\eta_1\|\boldsymbol{\beta}\|_2^2)}{(2+M\eta_1\|\boldsymbol{\beta}\|_2^2)^2}+\left(\frac{M\eta_1\|\boldsymbol{\beta}\|_2^2}{2+M\eta_1\|\boldsymbol{\beta}\|_2^2}\right)^2+\sum\limits_{k=L+1}^{K}\left[\ln\frac{4(1+M\eta_k)}{(2+M\eta_k)^2}+\left(\frac{M\eta_k}{2+M\eta_k}\right)^2\right]\right]}\mathcal{Q}\left(\sqrt{2T\left[\left(\frac{M\eta_1\|\boldsymbol{\beta}\|_2^2}{2+M\eta_1\|\boldsymbol{\beta}\|_2^2}\right)^2+\sum_{k=L+1}^{K}\left(\frac{M\eta_k}{2+M\eta_k}\right)^2\right]}\right) \tag{24}$$

$$\tilde{h} \approx \min\left[\sqrt{\frac{8T\mathbf{1}_K^{\mathrm{T}}\boldsymbol{J}^{-1}\mathbf{1}_K}{K}\left[\left(\frac{M\eta_1\|\boldsymbol{\beta}\|_2^2}{2+M\eta_1\|\boldsymbol{\beta}\|_2^2}\right)^2+\sum_{k=L+1}^{K}\left(\frac{M\eta_k}{2+M\eta_k}\right)^2\right]}, \sqrt{K}\zeta\right]. \tag{31}$$

B. ZZB for Estimation with Permutation Ambiguity

In subsection IV-A, we generalize the ZZB derivation from single source to multiple sources by following the existing framework, which, however, still makes the obtained ZZB invalid especially in the *a priori* performance region. The reason is that, the ordering process is required by multiple DOA estimators for the elimination of the permutation ambiguity, which implicitly changes the *a priori* distribution of DOAs. First, to illustrate the effect of the permutation ambiguity on MSE calculation, we consider the following example.

Example 1: Assuming there are two signals impinging on the array from 30° and 45°, while their estimates are respectively 29° and 44°. Accordingly, the root MSE (RMSE) should be calculated as $\sqrt{\frac{(30^\circ-29^\circ)^2+(45^\circ-44^\circ)^2}{2}} = 1.00^\circ$. However, when permutation ambiguity occurs, the output of DOAs estimator becomes 44° and 29°, leading to a wrong RMSE of $\sqrt{\frac{(30^\circ-44^\circ)^2+(45^\circ-29^\circ)^2}{2}} \approx 15.03^\circ$.

Although permutation ambiguity is ubiquitous for DOAs estimator, its impact on the MSE calculation is more prominent in the asymptotic region. Generally speaking, in the asymptotic region, the estimates of DOAs are around the true values, which leads to a small estimation error. On the contrary, the farther away from the asymptotic region, the greater the estimation error is. Obviously, to obtain the correct MSE, the outputs of DOAs estimators $\hat{\boldsymbol{\theta}}$ should not be directly matched to the true DOAs $\boldsymbol{\theta}$ during MSE calculation. To eliminate the permutation ambiguity, the estimated DOAs and the true DOAs are respectively ordered in ascending order before calculating the MSE. As such, the MSE should be calculated as

$$\mathrm{MSE} = \frac{1}{K}\sum_{k=1}^{K}\mathbb{E}\left\{\left(\hat{\theta}_{(k)} - \theta_{(k)}\right)^2\right\}, \tag{33}$$

where $\hat{\theta}_{(k)}$ and $\theta_{(k)}$ are the k-th smallest order statistic in $\hat{\boldsymbol{\theta}}$ and $\boldsymbol{\theta}$, respectively. Here, the subscript (k) enclosed in parentheses indicates the k-th order statistic of the sample.

Although the ordering process enables an accurate MSE calculation in the asymptotic region, it simultaneously have an effect on the MSE outside the asymptotic region because it implicitly changes the *a priori* distribution of DOAs $\boldsymbol{\theta}$. Actually, different DOAs are naturally assumed to be independent with each other, but such an ordering process introduces an extra dependence between the DOAs, making the generalized ZZB derived in subsection IV-A still invalid outside the asymptotic region. For example, in the *a priori* performance region, each θ_k tends to be randomly estimated according to its *a priori* distribution $\theta_k \sim \mathcal{U}[\vartheta_{\min}, \vartheta_{\max}]$, and the MSE of θ_k should converge to its *a priori* variance $\sigma^2_{\theta_k}$. After the ordering process, $\theta_{(k)}$ tends to be randomly estimated in the range $[\theta_{(k-1)}, \theta_{(k+1)}]$[3] rather than in $[\vartheta_{\min}, \vartheta_{\max}]$, and the MSE of $\theta_{(k)}$ should converge to its *a priori* variance $\sigma^2_{\theta_{(k)}}$. Obviously, with the number of sources K increasing, the average range of $\theta_{(k)}$ becomes narrower compared with the original θ_k, making the MSE scale down in the *a priori* performance region due to the ordering process.

[3]If $k=1$, the range becomes $[\vartheta_{\min}, \theta_{(2)}]$.

According to aforementioned discussion, the effect of ordering process on the MSE calculation can be formulated as the scale of between the traces of *a priori* covariance matrix of $\boldsymbol{\theta}$ before and after the ordering process, where the MSE scale factor is defined as

$$\kappa = \frac{\mathrm{Tr}\{\boldsymbol{R}_{(\boldsymbol{\theta})}\}}{\mathrm{Tr}\{\boldsymbol{R}_{\boldsymbol{\theta}}\}}. \tag{34}$$

Here,

$$\mathrm{Tr}\{\boldsymbol{R}_{(\boldsymbol{\theta})}\} = \sum_{k=1}^{K}\sigma^2_{\theta_{(k)}} \tag{35}$$

is the trace of the *a priori* covariance matrix of the order statistics $\{\theta_{(1)}, \cdots, \theta_{(K)}\}$.

According to the *a priori* PDF of $\theta_{(k)}$ [43, p.229]

$$f(\theta_{(k)}) = \frac{K!\left(\frac{\theta_{(k)}}{\zeta}\right)^{k-1}\left(1-\frac{\theta_{(k)}}{\zeta}\right)^{K-k}}{\zeta(k-1)!(K-k)!} \tag{36}$$

with $n!$ denoting the factorial of a non-negative integer n, the *a priori* variance of $\theta_{(k)}$ is

$$\begin{aligned}\sigma^2_{\theta_{(k)}} &= \int_0^{\zeta}\left(\theta_{(k)} - \mathbb{E}\left\{\theta_{(k)}\right\}\right)^2 f(\theta_{(k)})d\theta_{(k)} \\ &= \frac{\zeta^2(K+1-k)k}{(K+1)^2(K+2)},\end{aligned} \tag{37}$$

where

$$\mathbb{E}\left\{\theta_{(k)}\right\} = \int_0^{\zeta}\theta_{(k)} f(\theta_{(k)})d\theta_{(k)} = \frac{k\zeta}{K+1} \tag{38}$$

is the mean value. Thus, (35) becomes

$$\mathrm{Tr}\{\boldsymbol{R}_{(\boldsymbol{\theta})}\} = \frac{K\zeta^2}{6(K+1)}, \tag{39}$$

and the MSE scale factor accordingly becomes

$$\kappa = \frac{2}{K+1}, \tag{40}$$

which is a function of K, the number of sources. For single source case (i.e., $K=1$), we have $\kappa = 1$, namely, there is no permutation ambiguity. Furthermore, the MSE scale factor gets smaller with the number of sources increasing, indicating that the MSE gets more scale down in the *a priori* performance region after the ordering process. The reason is that, the average range $[\theta_{(k-1)}, \theta_{(k+1)}]$ gets narrower with the number of sources increasing.

In order to make the ZZB effective in the *a priori* performance region for multiple sources DOA estimation, we incorporate the MSE scale factor into (32) to obtain the final ZZB expression as

$$\mathrm{MSE} \geq 2P_{\mathrm{L}}\frac{K\zeta^2}{(K+1)^2(K+2)} + \Gamma_{\frac{3}{2}}(\tilde{u})\frac{\mathrm{Tr}\{\boldsymbol{J}^{-1}\}}{K}. \tag{41}$$

Obviously, as an explicit function of the number of sources, the derived ZZB is appropriate for multiple sources case. Besides, the ZZB also depends on the number of snapshots, the number of array sensors, SNRs of sources, *a priori* distribution of DOAs, array observation data via the Fisher information, and the coherent coefficient $\boldsymbol{\beta}$.

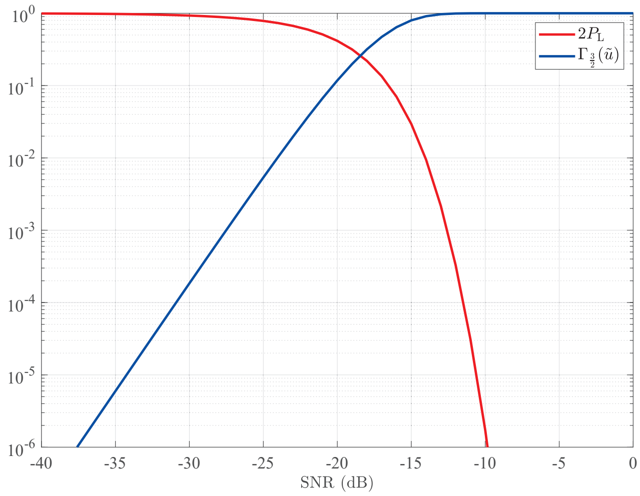

Fig. 1. Combination coefficients versus the SNR for single source.

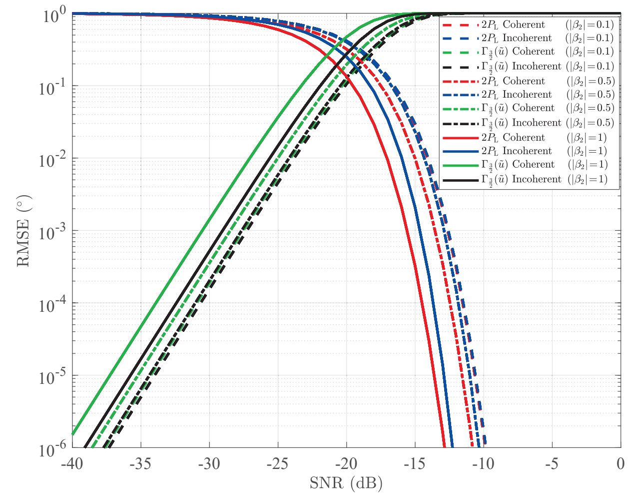

Fig. 2. Combination coefficients versus the SNR for two sources with different coherent coefficients.

In the *a priori* performance region, the derived ZZB converges to the *a priori* bound (APB) as

$$\lim_{\forall \eta_k \to 0} \text{MSE} = \frac{K\zeta^2}{(K+1)^2(K+2)}, \tag{42}$$

since

$$\lim_{\forall \eta_k \to 0} 2P_{\mathrm{L}} = 1, \tag{43}$$

and

$$\lim_{\forall \eta_k \to 0} \Gamma_{\frac{3}{2}}(\tilde{u}) = 0. \tag{44}$$

Obviously, the estimation accuracy of DOA estimators cannot be further improved by simply increasing the number of array sensors and/or the number of snapshots when the SNR tends to zero. In the asymptotic region, the derived ZZB converges to the CRB as

$$\lim_{\forall \eta_k \to +\infty} \text{MSE} = \frac{\mathrm{Tr}\{\boldsymbol{J}^{-1}\}}{K}, \tag{45}$$

since

$$\lim_{\forall \eta_k \to +\infty} 2P_{\mathrm{L}} = 0 \tag{46}$$

and

$$\lim_{\forall \eta_k \to +\infty} \Gamma_{\frac{3}{2}}(\tilde{u}) = 1. \tag{47}$$

Now it is clear that, the derived ZZB in (41) is a linear combination between the APB and the CRB, whose coefficients are $2P_{\mathrm{L}}$ and $\Gamma_{\frac{3}{2}}(\tilde{u})$, respectively.

For fully incoherent sources (say, $L=1$), P_{L} (24) and $\tilde{u}$ (30) respectively degrade to

$$P_{\mathrm{L}} = e^{T\sum_{k=1}^{K}\left[\ln\frac{4(1+M\eta_k)}{(2+M\eta_k)^2}+\left(\frac{M\eta_k}{2+M\eta_k}\right)^2\right]} \mathcal{Q}\left(\sqrt{2T\sum_{k=1}^{K}\left(\frac{M\eta_k}{2+M\eta_k}\right)^2}\right), \tag{48}$$

and

$$\tilde{u} \approx \min\left[\sqrt{T\sum_{k=1}^{K}\left(\frac{M\eta_k}{2+M\eta_k}\right)^2}, \frac{K^2\zeta^2}{8\mathbf{1}_K^{\mathrm{T}}\boldsymbol{J}^{-1}\mathbf{1}_K}\right]. \tag{49}$$

When K sources have the same SNR η, P_{L} and $\tilde{u}$ further become

$$P_{\mathrm{L}} = e^{KT\left[\ln\frac{4(1+M\eta)}{(2+M\eta)^2}+\left(\frac{M\eta}{2+M\eta}\right)^2\right]} \mathcal{Q}\left(\frac{\sqrt{2KT}M\eta}{2+M\eta}\right), \tag{50}$$

and

$$\tilde{u} \approx \min\left[KT\left(\frac{M\eta}{2+M\eta}\right)^2, \frac{K^2\zeta^2}{8\mathbf{1}_K^{\mathrm{T}}\boldsymbol{J}^{-1}\mathbf{1}_K}\right]. \tag{51}$$

Furthermore, when $K=1$, the ZZB is simplified to

$$\begin{aligned}&\mathbb{E}\left\{\left(\hat{\theta}-\theta\right)^2\right\}\\ &\geq 2e^{T\left[\ln\frac{4(1+M\eta)}{(2+M\eta)^2}+\left(\frac{M\eta}{2+M\eta}\right)^2\right]} \mathcal{Q}\left(\frac{\sqrt{2T}M\eta}{2+M\eta}\right)\sigma_\theta^2 + \Gamma_{\frac{3}{2}}(\tilde{u})\, J^{-1},\end{aligned} \tag{52}$$

where $\sigma_\theta^2 = \frac{\zeta^2}{12}$ denotes the *a priori* variance of θ. It is worth pointing out that, the ZZB (52) is consistent with the one [37, Eq. (C.30)], if we ignore the implicit condition $\tilde{h} < \sqrt{K}\zeta$ such that

$$\tilde{u} \approx T\left(\frac{M\eta}{2+M\eta}\right)^2, \tag{53}$$

and introduce the approximation [37, Eq. (C.14)].

In Fig. 1, we compare both combination coefficients versus the SNR, where a single source is assumed to follow *a priori* distribution $\mathcal{U}[-60^\circ, 60^\circ]$ w.r.t. a uniform linear array (ULA) consisting of $M=20$ sensors. The number of snapshots is fixed to $T=40$, and each SNR point is averaged over $10,000$ Monte-Carlo trials. It is observed that the coefficient $2P_{\mathrm{L}}$ decreases from 1 in the *a priori* performance region to 0 in the asymptotic region as expected, while the coefficient $\Gamma_{\frac{3}{2}}(\tilde{u})$ has the opposite trend. That is to say, the APB dominates the ZZB in the *a priori* performance region, but sharply vanishes in the asymptotic region. On the contrary, the CRB is ignorable in the *a priori* performance region, but gradually dominates the ZZB from the transition region to the asymptotic region.

Unlike the single source case, both the combination coefficients $2P_{\mathrm{L}}$ and $\Gamma_{\frac{3}{2}}(\tilde{u})$ also depend on the coherent coefficient $\boldsymbol{\beta}$ under coherent multiple sources case. Hence, in Fig. 2,

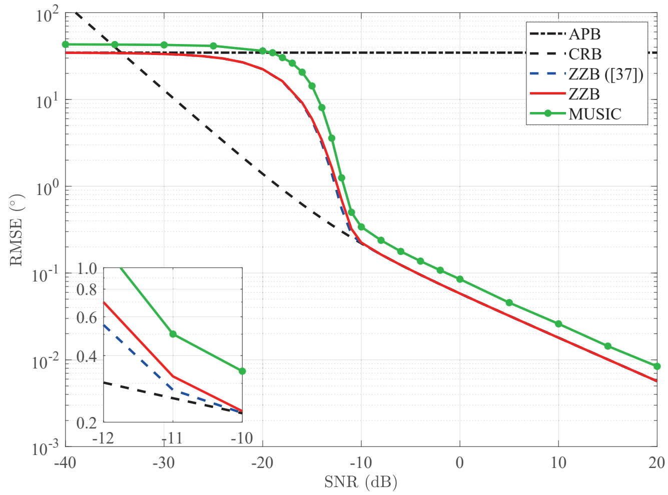

Fig. 3. Comparison of bounds and MUSIC performance for single source case ($K = 1$).

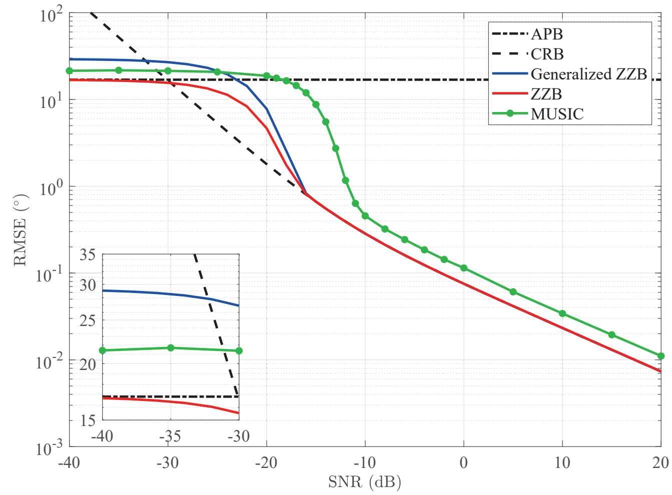

Fig. 4. Comparison of bounds and MUSIC performance for multiple sources case ($K = 5$).

we compare both the combination coefficients versus the SNR with two coherent sources, where different coherent coefficients β_2 are considered. Meanwhile, the corresponding combination coefficients for incoherent sources are also plotted as reference, where the second source is independent of the first one with the power $\sigma_2^2 = |\beta_2|^2\sigma_1^2$. It is observed from Fig. 2 that, the difference between the coherent and incoherent combination coefficients becomes larger with the coherent coefficient β_2 increasing. The reason is that, larger β_2 leads to larger norm $\|\boldsymbol{\beta}\|_2^2$ in (24) and (31), which makes the combination coefficients $2P_{\mathrm{L}}$ and $\Gamma_{\frac{3}{2}}(\tilde{u})$ in coherent case more distinguishable from those in incoherent case. On the other hand, with β_2 increasing, $2P_{\mathrm{L}}$ and $\Gamma_{\frac{3}{2}}(\tilde{u})$ respectively decreases from 1 and reaches to 1 at lower SNR, indicating that the ZZB will leave the *a priori* performance region and will enter the asymptotic region faster. Furthermore, for the same β_2, $2P_{\mathrm{L}}$ and $\Gamma_{\frac{3}{2}}(\tilde{u})$ in coherent case respectively decreases from 1 and reaches to 1 earlier than those in incoherent case, indicating that the coherent ZZB will leave from the APB and touch the CRB earlier than in incoherent ZZB.

Remark: For underdetermined DOAs estimation (say, $K > M$) using virtual coarray, the $\imath\jmath$-th entry of Fisher information matrix w.r.t. $\boldsymbol{\theta}$ is

$$\boldsymbol{J}_{\imath\jmath} = T\left[\mathrm{vec}\left(\frac{\partial \boldsymbol{R}_{\boldsymbol{x}|\boldsymbol{\theta}}}{\partial \theta_\imath}\right)\right]^{\mathrm{H}}\left(\boldsymbol{R}_{\boldsymbol{x}|\boldsymbol{\theta}}^{\mathrm{T}} \otimes \boldsymbol{R}_{\boldsymbol{x}|\boldsymbol{\theta}}\right)^{-1}\mathrm{vec}\left(\frac{\partial \boldsymbol{R}_{\boldsymbol{x}|\boldsymbol{\theta}}}{\partial \theta_\jmath}\right) \quad (54)$$

according to [19, Eq. 37], such that the rank defect problem is avoided. Here, $\mathrm{vec}(\cdot)$ denotes the vectorization operator, and $\otimes$ represents Kronecker product. Thus, the derived ZZB provides a unified expression for both overdetermined and underdetermined DOAs estimation.

V. Simulations

In this section, we evaluate the derived ZZB for multiple sources DOA estimation, where the CRB is also plotted for a reference. Since ZZB requires the *a priori* distribution, we assume each DOA to follow a uniform distribution as $\mathcal{U}[-60°, 60°]$ in our simulations. We run $\mathcal{L} = 10,000$ Monte-Carlo trials for each data point (SNR) to obtain the involved bounds and the RMSE of DOAs estimation. Here, the RMSE is defined as

$$\mathrm{RMSE} = \sqrt{\frac{1}{\mathcal{L}K}\sum_{\ell=1}^{\mathcal{L}}\sum_{k=1}^{K}\left(\hat{\theta}_{\ell,(k)} - \theta_{\ell,(k)}\right)^2}, \quad (55)$$

where $\hat{\theta}_{\ell,(k)}$ is the estimate of $\theta_{\ell,(k)}$, the k-th DOA after ordering process for the ℓ-th Monte-Carlo trial. To keep sources resolvable, we assume a minimum interval of $10°$ in each $\boldsymbol{\theta}$ in multiple sources case, i.e., K DOAs in each trial are sampled with at least $10°$ separation. Note that, according to (41), the derived ZZB is of course appropriate for multiple sources with different SNRs. Although any linear array configuration is applicable, here we adopt the ULA with $M = 20$ sensors, where the spacing between sensors is half wavelength. Unless otherwise specified, the number of snapshots is fixed to $T = 40$ in our simulations.

Considering that the ZZB in [37] is only appropriate for the single source case, we first compare derived ZZB with the ZZB in [37] under the single source assumption. Meanwhile, the APB, and the MUSIC algorithm are also plotted for the reference. It is observed from Fig. 3 that, due to the extra approximation [37, Eq. (C.14)], the ZZB in [37] achieves the asymptotic region at a slightly lower input SNR than the derived ZZB (52), which is similar with the comparison between the ZZB in [37] and its numerical integration (see, [37, Fig. 4]). Besides that, the derived ZZB and the ZZB in [37] are consistent with the APB in the *a priori* performance region, and are consistent with the CRB in the asymptotic region. Furthermore, the ZZB provides a tighter bound than the CRB outside the asymptotic region, and also predicts the threshold entering the asymptotic region for DOA estimation algorithms (e.g., MUSIC). On the contrary, since no *a priori* information is used, the CRB provides a loose bound outside the asymptotic region, and finally divergence exceeds the MSE of MUSIC algorithm in the *a priori* performance region.

Then, we evaluate the derived ZZB under fully incoherent multiple sources assumption, where all K sources are assumed to have the same SNRs. It is observed from Fig. 4 that, the

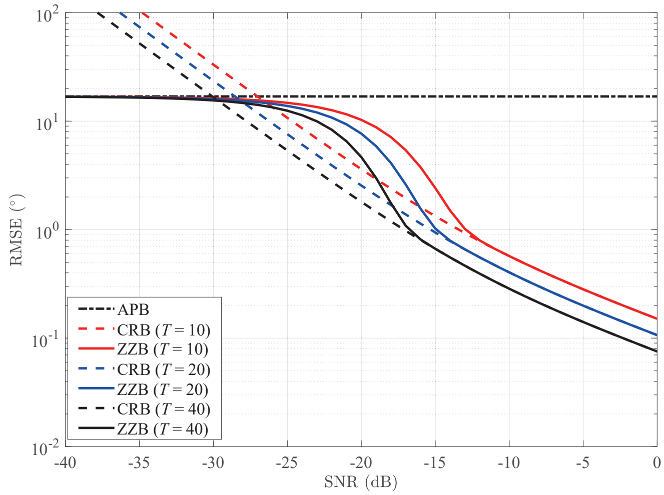

Fig. 5. Effect of the number of snapshots T on ZZB.

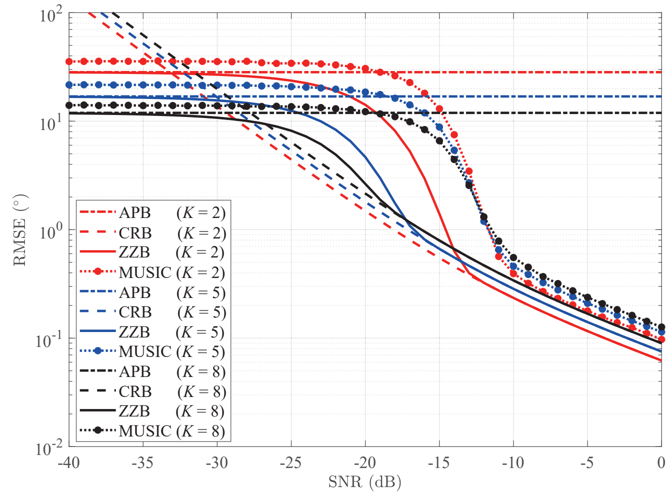

Fig. 6. Effect of the number of sources K on ZZB.

generalized ZZB and the derived ZZB achieve the asymptotic region at the same SNR, then keep consistent with the CRB in the asymptotic region. However, below the asymptotic region threshold, the generalized ZZB increases faster than the derived ZZB before entering the *a priori* performance region, and finally convergence exceeds the MSE of MUSIC algorithm. The CRB still provides a loose bound in the transition region, and finally divergence exceeds the MSE of MUSIC algorithm, which is the same as single source case. On the contrary, benefited from the scale factor κ (40) considering the ordering process required in multiple sources DOA estimation, the derived ZZB is consistently lower than the generalized ZZB outside the asymptotic region, and is effective to lower bound the MSE of the MUSIC algorithm in the *a priori* performance region. As predicted, the derived ZZB converges to the APB in the *a priori* performance region. Hence, the derived ZZB provides a global lower bound tighter than CRB for multiple sources DOA estimation. Furthermore, the asymptotic region threshold for the ZZB in Fig. 4 appears at a lower SNR than that in Fig. 3, which is because the coefficients $2P_{\mathrm{L}}$ and $\Gamma_{\frac{3}{2}}(\tilde{u})$ respectively converge to 0 and 1 more sharply with K increasing.

Obviously, the derived ZZB is the function of the number of snapshots T. Hence, we investigate the effect of the number of snapshots T on the derived ZZB, where the number of sources is fixed to $K = 5$. It is observed from Fig. 5 that, the ZZBs converge together to the APB in the *a priori* performance region regardless of the number of snapshots. This is because the MSE convergency performance in the *a priori* performance region only depends on the *a priori* distribution of DOAs and the number of sources. Nevertheless, we prefer more snapshots to bring the lower bound when operating outside the *a priori* performance region, which implies the better estimation performance. Specifically, with the increase of T, the ZZB reaches the CRB at a lower SNR, leading to a wider asymptotic region and a narrower transition region. Each double snapshots brings a fixed decrease of the threshold point, which helps predict the asymptotic region threshold of the ZZB under different snapshots.

We also evaluate the effect of number of sources K on the derived ZZB in Fig. 6. It is observed that, for different number of sources K, the derived ZZB always effectively lower bounds the corresponding MSE of the MUSIC algorithm, and respectively converges to the corresponding APB (42) in the *a priori* performance region and CRB in the asymptotic region. With the number of source K increasing, the derived ZZB touches the corresponding CRB at a lower SNR, since the monotonic augmentation function $\Gamma_{\frac{3}{2}}(\tilde{u})$ (30) w.r.t. K converges to 1 (i.e., ZZB converges to CRB) faster. Meanwhile, the derived ZZB converges to a lower APB in the *a priori* performance region and a higher CRB in the asymptotic region, such that the difference between ZZB and the corresponding CRB in the transition region becomes narrower. Even so, ZZB always converges to APB with SNR decreasing, while CRB becomes invalid to evaluate the estimation performance of DOA estimator (e.g., MUSIC) in low SNR situation.

Now, we evaluate the derived ZZB for coherent DOA estimation. We assume there are $K = 5$ sources signals impinging on the ULA, where the first $L = 3$ signals are mutually coherent with the coefficient $\boldsymbol{\beta} = [1, 0.9e^{j\phi_1}, 0.8e^{j\phi_2}]$, whereas the last 2 signals are incoherent. Here, ϕ_1 and ϕ_2 are random phases following a uniform distribution $\mathcal{U}[-\pi, \pi]$. Also we compare coherent ZZB with incoherent ZZB, where corresponding CRBs [16] are also plotted as references. For fair comparison, the SNRs of 5 sources in the fully incoherent sources scenario are $\eta_2 = |\beta_2|^2\eta_1$, $\eta_3 = |\beta_3|^2\eta_1$, $\eta_4 = \eta_5 = \eta_1$, respectively. Other simulation conditions are same as those in Fig. 4. It is observed from Fig. 7 that, both coherent ZZB and incoherent ZZB are consistent with APB in the low SNR situation, which indicates that, whether coherent or not does not affect the ZZB in such a low SNR region. On the other hand, both coherent ZZB and incoherent ZZB converge to the corresponding CRB in the asymptotic region. However, the coherent ZZB is lower than incoherent ZZB in the transition region. The reason is that, the ZZB is a linear combination between the APB and CRB, where $2P_{\mathrm{L}}$ in coherent ZZB decreases from 1 faster than that in incoherent ZZB (as shown in Fig. 2), making the coherent ZZB decreases from the APB

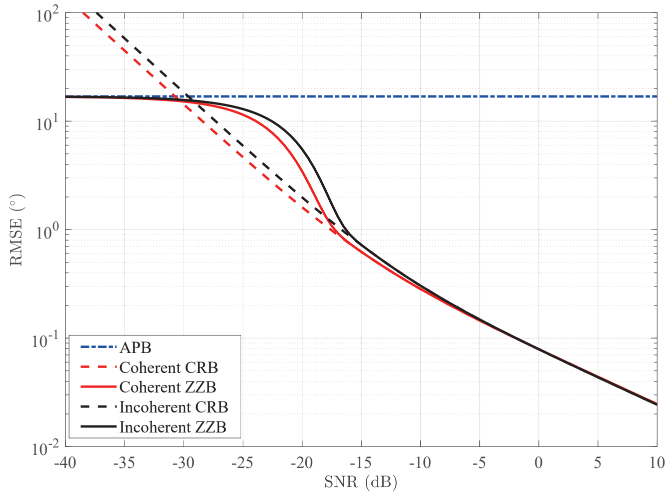

Fig. 7. Comparison between coherent ZZB and incoherent ZZB.

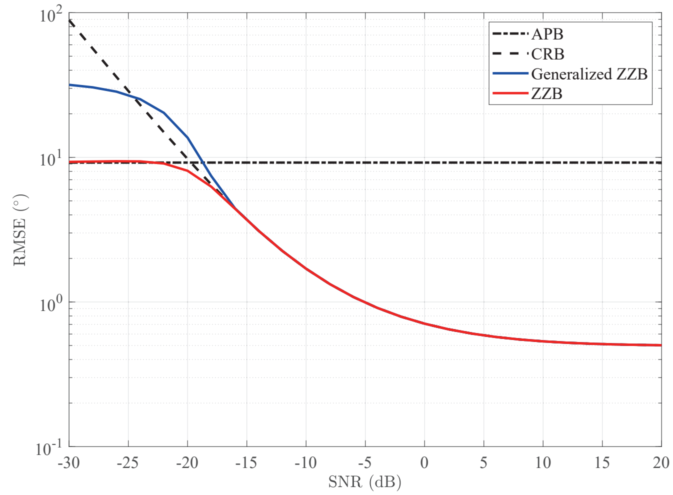

Fig. 8. ZZB for underdetermined DOA estimation.

faster. Thus, the coherent ZZB is lower than the incoherent ZZB.

In addition to the overdetermined DOA estimation, the derived ZZB is also appropriate for the underdetermined DOA estimation by incorporating the coarray Fisher information. Unlike the aforementioned ULA, we adopt a $(3, 5)$ pair coprime linear array (the number of array sensors $M = 2 \times 3 + 5 - 1 = 10$) [44, 45] to estimate $K = 11$ DOAs following the same *a priori* distribution $\mathcal{U}[-60°, 60°]$ with the minimum interval of $5°$. Both the coarray CRB [19, Eq. 37] and the generalized ZZB are plotted for comparison. All the sources are assumed to be fully incoherent with the same SNR. It is observed from Fig. 8 that, the derived ZZB converges to the coarray CRB in the asymptotic region, and also flatten out as predicted when the SNR gets higher. On the other hand, the derived ZZB converges to the APB as predicted in the *a priori* performance region. Hence, the derived ZZB also provides a unified bound for underdetermined DOAs estimation from the *a priori* performance region to the asymptotic region.

VI. Conclusions

In this paper, we derived an explicit ZZB for hybrid coherent/incoherent multiple sources DOA estimation as a function of the number of sources, the number of array sensors, the number of snapshots, the *a priori* distribution and SNRs of sources, array observation data, and the coherent coefficient. Different from the single source DOA estimation, the ordering process for eliminating permutation ambiguity during MSE calculation of multiple sources DOA estimation still makes the generalized ZZB invalid outside the asymptotic region. Hence, we for the first time introduced the order statistics to describe the effect of the ordering process on the ZZB, and further made the derived ZZB keep global tight for evaluating the MSE of multiple sources DOA estimation. It is noted that, the derived ZZB also provided a unified bound for both overdetermined DOA estimation and underdetermined DOA estimation. Besides, the derived ZZB for the first time revealed the relationship between the MSE convergence performance and the number of sources, regardless of the number of snapshots and the linear array configuration. Simulation results demonstrate the advantages of the derived ZZB over the CRB in a wider range of SNR. We notice that, in the transition region, the derived ZZB may be affected by Fisher information when some sources are closely located, which will be studied in future work. Finally, although the ZZB is derived for DOAs estimation with a linear array, we believe that the basic conclusions are valid for two-dimensional DOA estimation and other discrete vector parameter estimation problems with permutation ambiguity.

Appendix A
Derivation of $\mu(p;\boldsymbol{\delta})|_{p=\frac{1}{2}}$ and $\frac{\partial^2\mu(p;\boldsymbol{\delta})}{\partial p^2}\big|_{p=\frac{1}{2}}$

For completeness, we generalize the derivation for single source in [37] to multiple sources case. For the observation data matrix $\boldsymbol{X}$ with T snapshots, $\mu(p;\boldsymbol{\delta})$ is explicitly expressed as [41, p. 67]

$$\begin{aligned}\mu(p;\boldsymbol{\delta}) = T\big[&p\ln|\boldsymbol{R}_{\boldsymbol{x}|\boldsymbol{\varphi}}| + (1-p)\ln|\boldsymbol{R}_{\boldsymbol{x}|\boldsymbol{\varphi}+\boldsymbol{\delta}}| \\ &- \ln|p\boldsymbol{R}_{\boldsymbol{x}|\boldsymbol{\varphi}} + (1-p)\boldsymbol{R}_{\boldsymbol{x}|\boldsymbol{\varphi}+\boldsymbol{\delta}}|\big],\end{aligned} \tag{56}$$

where $\boldsymbol{R}_{\boldsymbol{x}|\boldsymbol{\varphi}} \triangleq \boldsymbol{R}_{\boldsymbol{x}|\boldsymbol{\theta}=\boldsymbol{\varphi}}$ and $\boldsymbol{R}_{\boldsymbol{x}|\boldsymbol{\varphi}+\boldsymbol{\delta}} \triangleq \boldsymbol{R}_{\boldsymbol{x}|\boldsymbol{\theta}=\boldsymbol{\varphi}+\boldsymbol{\delta}}$. Here, $|\cdot|$ represents the determinant of a matrix.

The first derivative of $\mu(p;\boldsymbol{\delta})$ w.r.t. p is

$$\begin{aligned}\frac{\partial\mu(p;\boldsymbol{\delta})}{\partial p} = T\Big[&\ln|\boldsymbol{R}_{\boldsymbol{x}|\boldsymbol{\varphi}}| - \ln|\boldsymbol{R}_{\boldsymbol{x}|\boldsymbol{\varphi}+\boldsymbol{\delta}}| \\ &- \mathrm{Tr}\Big\{\big[p\boldsymbol{R}_{\boldsymbol{x}|\boldsymbol{\varphi}} + (1-p)\boldsymbol{R}_{\boldsymbol{x}|\boldsymbol{\varphi}+\boldsymbol{\delta}}\big]^{-1}\boldsymbol{R}_{-}\Big\}\Big]\end{aligned} \tag{57}$$

by denoting $\boldsymbol{R}_{-} = \boldsymbol{R}_{\boldsymbol{x}|\boldsymbol{\varphi}} - \boldsymbol{R}_{\boldsymbol{x}|\boldsymbol{\varphi}+\boldsymbol{\delta}}$, and then the second derivative of $\mu(p;\boldsymbol{\delta})$ w.r.t. p is

$$\frac{\partial^2\mu(p;\boldsymbol{\delta})}{\partial p^2} = T\mathrm{Tr}\Big\{\Big[\big[p\boldsymbol{R}_{\boldsymbol{x}|\boldsymbol{\varphi}} + (1-p)\boldsymbol{R}_{\boldsymbol{x}|\boldsymbol{\varphi}+\boldsymbol{\delta}}\big]^{-1}\boldsymbol{R}_{-}\Big]^2\Big\}. \tag{58}$$

Hence, by denoting $\boldsymbol{R}_{+} = \boldsymbol{R}_{\boldsymbol{x}|\boldsymbol{\varphi}} + \boldsymbol{R}_{\boldsymbol{x}|\boldsymbol{\varphi}+\boldsymbol{\delta}}$, $\mu(p;\boldsymbol{\delta})|_{p=\frac{1}{2}}$ and $\frac{\partial^2\mu(p;\boldsymbol{\delta})}{\partial p^2}\big|_{p=\frac{1}{2}}$ respectively become

$$\mu(p;\boldsymbol{\delta})|_{p=\frac{1}{2}} = T\left[\frac{\ln\big(|\boldsymbol{R}_{\boldsymbol{x}|\boldsymbol{\varphi}}||\boldsymbol{R}_{\boldsymbol{x}|\boldsymbol{\varphi}+\boldsymbol{\delta}}|\big)}{2} - \ln\left|\frac{\boldsymbol{R}_{+}}{2}\right|\right], \tag{59}$$

and

$$\left.\frac{\partial^2\mu(p;\boldsymbol{\delta})}{\partial p^2}\right|_{p=\frac{1}{2}} = 4T\mathrm{Tr}\left\{\left(\boldsymbol{R}_+^{-1}\boldsymbol{R}_-\right)^2\right\}. \tag{60}$$

By performing the second-order Taylor series expansion of $\mu(p;\boldsymbol{\delta})|_{p=\frac{1}{2}}$ and $\frac{\partial^2\mu(p;\boldsymbol{\delta})}{\partial p^2}|_{p=\frac{1}{2}}$ around the point $\boldsymbol{\delta}=\boldsymbol{0}_K$, we have

$$\mu(p;\boldsymbol{\delta})|_{p=\frac{1}{2}} \approx -\frac{1}{8}\boldsymbol{\delta}^{\mathrm{T}}\boldsymbol{J}\boldsymbol{\delta}, \tag{61}$$

and

$$\left.\frac{\partial^2\mu(p;\boldsymbol{\delta})}{\partial p^2}\right|_{p=\frac{1}{2}} \approx \boldsymbol{\delta}^{\mathrm{T}}\boldsymbol{J}\boldsymbol{\delta}. \tag{62}$$

Thus, by substituting (61) and (62) into (16), $P(\boldsymbol{\delta})$ is approximated as $P_{\mathrm{S}}(\boldsymbol{\delta})$ given in (23). Although the result is consistent with [37, Eq. (D. 12)], the derivation here is generalized to multiple sources case because there is no single source assumption required.

Since the approximation $P(\boldsymbol{\delta})\approx P_{\mathrm{S}}(\boldsymbol{\delta})$ is only appropriate for $\boldsymbol{\delta}$ located in a region Δ around $\boldsymbol{0}_K$, we further investigate (16) for $\boldsymbol{\delta}$ outside the region Δ. According to Sylvester's determinant theorem

$$|\boldsymbol{I}_M+\boldsymbol{U}\boldsymbol{V}| = |\boldsymbol{I}_K+\boldsymbol{V}\boldsymbol{U}| \tag{63}$$

for $\boldsymbol{U}\in\mathbb{C}^{M\times K}$ and $\boldsymbol{V}\in\mathbb{C}^{K\times M}$, the determinants in (59) can be respectively written as

$$|\boldsymbol{R}_{\boldsymbol{x}|\boldsymbol{\varphi}}| = \sigma_n^{2M}\left|\boldsymbol{I}_K+\frac{1}{\sigma_n^2}\boldsymbol{A}^{\mathrm{H}}(\boldsymbol{\varphi})\boldsymbol{A}(\boldsymbol{\varphi})\boldsymbol{\Sigma}\right|, \tag{64}$$

$$|\boldsymbol{R}_{\boldsymbol{x}|\boldsymbol{\varphi}+\boldsymbol{\delta}}| = \sigma_n^{2M}\left|\boldsymbol{I}_K+\frac{1}{\sigma_n^2}\boldsymbol{A}^{\mathrm{H}}(\boldsymbol{\varphi}+\boldsymbol{\delta})\boldsymbol{A}(\boldsymbol{\varphi}+\boldsymbol{\delta})\boldsymbol{\Sigma}\right|, \tag{65}$$

and

$$\left|\frac{1}{2}\boldsymbol{R}_+\right| = \sigma_n^{2M}\left|\boldsymbol{I}_{2K}+\frac{1}{2\sigma_n^2}\boldsymbol{B}^{\mathrm{H}}\boldsymbol{B}\boldsymbol{D}\right|, \tag{66}$$

where

$$\boldsymbol{B} = [\boldsymbol{A}(\boldsymbol{\varphi}), \boldsymbol{A}(\boldsymbol{\varphi}+\boldsymbol{\delta})], \tag{67}$$

and

$$\boldsymbol{D} = \text{block diag}[\boldsymbol{\Sigma}_{co}, \boldsymbol{\Sigma}_{in}, \boldsymbol{\Sigma}_{co}, \boldsymbol{\Sigma}_{in}]. \tag{68}$$

Obviously, $\boldsymbol{A}^{\mathrm{H}}(\boldsymbol{\varphi})\boldsymbol{A}(\boldsymbol{\varphi})$, $\boldsymbol{A}^{\mathrm{H}}(\boldsymbol{\varphi}+\boldsymbol{\delta})\boldsymbol{A}(\boldsymbol{\varphi}+\boldsymbol{\delta})$, and $\boldsymbol{B}^{\mathrm{H}}\boldsymbol{B}$ are related to the array beampattern, whose null points coincide with the minima of $P(\boldsymbol{\delta})$. The null points of the array beampattern occur at

$$\left|\boldsymbol{a}^{\mathrm{H}}(\theta)\boldsymbol{a}(\theta+\delta)\right| = 0 \tag{69}$$

for single source case [37], which implies the steering vector $\boldsymbol{a}^{\mathrm{H}}(\theta+\delta)$ is orthogonal to $\boldsymbol{a}(\theta)$. By generalizing (69) for multiple source case, we propose the following approximation

$$\boldsymbol{A}^{\mathrm{H}}(\boldsymbol{\theta})\boldsymbol{A}(\boldsymbol{\theta}) \approx M\boldsymbol{I}_K, \boldsymbol{\theta}=\boldsymbol{\varphi}, \boldsymbol{\varphi}+\boldsymbol{\delta} \tag{70}$$

by considering that multiple steering vectors are approximately orthogonal to each other, from which we have[4]

$$\boldsymbol{B}^{\mathrm{H}}\boldsymbol{B} \approx M\boldsymbol{I}_{2K}. \tag{71}$$

As such, (59) can be approximated as

$$\begin{aligned}\mu(p;\boldsymbol{\delta})|_{p=\frac{1}{2}} &\approx T\ln\frac{\left|\boldsymbol{I}_K+\frac{M}{\sigma_n^2}\boldsymbol{\Sigma}\right|}{\left|\boldsymbol{I}_{2K}+\frac{M}{2\sigma_n^2}\boldsymbol{D}\right|}\\ &= T\ln\frac{\left|\boldsymbol{I}_L+\frac{M}{\sigma_n^2}\boldsymbol{\Sigma}_{co}\right|\left|\boldsymbol{I}_{K-L}+\frac{M}{\sigma_n^2}\boldsymbol{\Sigma}_{in}\right|}{\left|\boldsymbol{I}_L+\frac{M}{2\sigma_n^2}\boldsymbol{\Sigma}_{co}\right|^2\left|\boldsymbol{I}_{K-L}+\frac{M}{2\sigma_n^2}\boldsymbol{\Sigma}_{in}\right|^2}\\ &= T\ln\frac{4(1+M\eta_1\|\boldsymbol{\beta}\|_2^2)}{(2+M\eta_1\|\boldsymbol{\beta}\|_2^2)^2}+T\sum_{k=L+1}^{K}\ln\frac{4(1+M\eta_k)}{(2+M\eta_k)^2}.\end{aligned} \tag{72}$$

Then, $\boldsymbol{R}_+$ and $\boldsymbol{R}_-$ in (60) can be further written as

$$\boldsymbol{R}_+ = 2\sigma_n^2\boldsymbol{I}_M+\boldsymbol{B}\boldsymbol{D}\boldsymbol{B}^{\mathrm{H}}, \tag{73}$$

and

$$\boldsymbol{R}_- = \boldsymbol{B}\tilde{\boldsymbol{D}}\boldsymbol{B}^{\mathrm{H}}, \tag{74}$$

respectively, where

$$\tilde{\boldsymbol{D}} = \text{block diag}[\boldsymbol{\Sigma}_{co}, \boldsymbol{\Sigma}_{in}, -\boldsymbol{\Sigma}_{co}, -\boldsymbol{\Sigma}_{in}]. \tag{75}$$

According to Woodbury matrix identity, the inverse of $\boldsymbol{R}_+$ can be approximated as

$$\boldsymbol{R}_+^{-1} \approx \frac{1}{2\sigma_n^2}\boldsymbol{I}_M-\frac{1}{4\sigma_n^4}\boldsymbol{B}\boldsymbol{D}\boldsymbol{Y}\boldsymbol{B}^{\mathrm{H}} \tag{76}$$

with the approximation condition (71), where

$$\begin{aligned}\boldsymbol{Y} &= \left(\boldsymbol{I}_{2K}+\frac{M}{2\sigma_n^2}\boldsymbol{D}\right)^{-1}\\ &= \text{block diag}[\boldsymbol{Y}_{co}, \boldsymbol{Y}_{in}, \boldsymbol{Y}_{co}, \boldsymbol{Y}_{in}]\end{aligned} \tag{77}$$

with

$$\begin{aligned}\boldsymbol{Y}_{co} &= \left(\boldsymbol{I}_L+\frac{M}{2\sigma_n^2}\boldsymbol{\Sigma}_{co}\right)^{-1}\\ &= \boldsymbol{I}_L-\frac{M\eta_1}{2+M\eta_1\|\boldsymbol{\beta}\|_2^2}\boldsymbol{\beta}\boldsymbol{\beta}^{\mathrm{H}}\end{aligned} \tag{78}$$

according to Sherman-Morrison formula, and

$$\begin{aligned}\boldsymbol{Y}_{in} &= \left(\boldsymbol{I}_{K-L}+\frac{M}{2\sigma_n^2}\boldsymbol{\Sigma}_{in}\right)^{-1}\\ &= \mathrm{diag}\left[\left(1+\frac{M\eta_{L+1}}{2}\right)^{-1}, \cdots, \left(1+\frac{M\eta_K}{2}\right)^{-1}\right].\end{aligned} \tag{79}$$

Accordingly, we have

$$\begin{aligned}&(\boldsymbol{R}_+^{-1}\boldsymbol{R}_-)^2\\ &\approx \frac{M}{4\sigma_n^4}\left(\boldsymbol{B}\boldsymbol{D}^2\boldsymbol{B}^{\mathrm{H}}-\frac{M}{\sigma_n^2}\boldsymbol{B}\boldsymbol{D}^3\boldsymbol{Y}\boldsymbol{B}^{\mathrm{H}}+\frac{M^2}{4\sigma_n^4}\boldsymbol{B}\boldsymbol{D}^4\boldsymbol{Y}^2\boldsymbol{B}^{\mathrm{H}}\right)\end{aligned} \tag{80}$$

since

$$\boldsymbol{D}^2 = \tilde{\boldsymbol{D}}^2. \tag{81}$$

Then, (60) is approximated as

$$\left.\frac{\partial^2\mu(p;\boldsymbol{\delta})}{\partial p^2}\right|_{p=\frac{1}{2}} \approx \frac{TM^2}{\sigma_n^4}\mathrm{Tr}\left\{\left(\boldsymbol{D}^2-\frac{M}{\sigma_n^2}\boldsymbol{D}^3\boldsymbol{Y}+\frac{M^2}{4\sigma_n^4}\boldsymbol{D}^4\boldsymbol{Y}^2\right)\right\}, \tag{82}$$

where the trace of $\boldsymbol{D}^2$, $\boldsymbol{D}^3\boldsymbol{Y}$, and $\boldsymbol{D}^4\boldsymbol{Y}^2$ are respectively

[4] To obtain the minimum value of $P(\boldsymbol{\delta})$, we can only consider the case there is no same value in $\boldsymbol{\varphi}$ and $\boldsymbol{\varphi}+\boldsymbol{\delta}$, such that the steering vectors in $\boldsymbol{A}(\boldsymbol{\varphi})$ are also orthogonal to those $\boldsymbol{A}(\boldsymbol{\varphi}+\boldsymbol{\delta})$.

expressed as

$$\mathrm{Tr}\{\boldsymbol{D}^2\} = 2\sigma_1^4\|\boldsymbol{\beta}\|_2^4 + \sum_{k=L+1}^{K} 2\sigma_k^4, \tag{83}$$

$$\mathrm{Tr}\{\boldsymbol{D}^3\boldsymbol{Y}\} = \frac{4\sigma_1^6\|\boldsymbol{\beta}\|_2^6}{2+M\eta_1\|\boldsymbol{\beta}\|_2^2} + \sum_{k=L+1}^{K} \frac{4\sigma_k^6}{2+M\eta_k}. \tag{84}$$

and

$$\mathrm{Tr}\{\boldsymbol{D}^4\boldsymbol{Y}^2\} = \frac{8\sigma_1^8\|\boldsymbol{\beta}\|_2^8}{(2+M\eta_1\|\boldsymbol{\beta}\|_2^2)^2} + \sum_{k=L+1}^{K} \frac{8\sigma_k^8}{(2+M\eta_l)^2}. \tag{85}$$

Finally, (82) becomes

$$\left.\frac{\partial^2\mu(p;\boldsymbol{\delta})}{\partial p^2}\right|_{p=\frac{1}{2}} \approx 8T\left[\left(\frac{M\eta_1\|\boldsymbol{\beta}\|_2^2}{2+M\eta_1\|\boldsymbol{\beta}\|_2^2}\right)^2 + \sum_{k=L+1}^{K}\left(\frac{M\eta_k}{2+M\eta_k}\right)^2\right], \tag{86}$$

which is a function of SNR η_k, the number of array sensors M, the number of sources K and the coherent coefficient $\boldsymbol{\beta}$. By substituting (72) and (86) into (16), $P(\boldsymbol{\delta})$ for $\boldsymbol{\delta}$ outside the region Δ is approximated as P_{L}, which is given in (24).

The boundary of the region Δ occurs at $P_{\mathrm{S}}(\boldsymbol{\delta}) = P_{\mathrm{L}}$. However, the explicit boundary is difficult to calculate. Similar to [37], considering that $\mathcal{Q}(z)$ is a decreasing function w.r.t. z, the region Δ can be approximately given by

$$\frac{\sqrt{\boldsymbol{\delta}^{\mathrm{T}}\boldsymbol{J}\boldsymbol{\delta}}}{2} \le \sqrt{2T\left[\left(\frac{M\eta_1\|\boldsymbol{\beta}\|_2^2}{2+M\eta_1\|\boldsymbol{\beta}\|_2^2}\right)^2 + \sum_{k=L+1}^{K}\left(\frac{M\eta_k}{2+M\eta_k}\right)^2\right]}, \tag{87}$$

which is the interior of an ellipse given in (21).

Appendix B
Derivation of (27)

In this Appendix, we follow the framework in [37] to sovle the optimization problem in (14). It is worth noting that, in our derivation, $\boldsymbol{\theta}$ follows uniform *a priori* distribution, rather than defined on a subset of the unit disc in [37]. First, by substituting (22) into (25), we have

$$\begin{aligned} &P(\boldsymbol{\delta})\frac{\prod_{k=1}^{K}(\zeta-|\delta_k|)}{\zeta^K} \\ &\approx P_{\mathrm{L}}\frac{\prod_{k=1}^{K}(\zeta-|\delta_k|)}{\zeta^K} + \begin{cases} P_{\mathrm{S}}(\boldsymbol{\delta})-P_{\mathrm{L}} & \boldsymbol{\delta}\in\Delta \\ 0 & \boldsymbol{\delta}\notin\Delta \end{cases}, \end{aligned} \tag{88}$$

and thus the corresponding optimization problem in (14) can be divided into three separated terms as

$$\begin{aligned} &\max_{\boldsymbol{\delta}:\mathbf{1}_K^{\mathrm{T}}\boldsymbol{\delta}=\sqrt{K}h} P(\boldsymbol{\delta})\frac{\prod_{k=1}^{K}(\zeta-|\delta_k|)}{\zeta^K} \\ &\approx \max_{\boldsymbol{\delta}:\mathbf{1}_K^{\mathrm{T}}\boldsymbol{\delta}=\sqrt{K}h} P_{\mathrm{L}}\frac{\prod_{k=1}^{K}(\zeta-|\delta_k|)}{\zeta^K} + \max_{\boldsymbol{\delta}\in\Delta:\mathbf{1}_K^{\mathrm{T}}\boldsymbol{\delta}=\sqrt{K}h} P_{\mathrm{S}}(\boldsymbol{\delta})-P_{\mathrm{L}}. \end{aligned} \tag{89}$$

Then, we have the following property about the maximum of $\frac{\prod_{k=1}^{K}(\zeta-|\delta_k|)}{\zeta^K}$.

Property 1.

$$\max_{\boldsymbol{\delta}:\mathbf{1}_K^{\mathrm{T}}\boldsymbol{\delta}=\sqrt{K}h} \frac{\prod_{k=1}^{K}(\zeta-|\delta_k|)}{\zeta^K} = \left(1-\frac{h}{\zeta\sqrt{K}}\right)^K. \tag{90}$$

Proof: Obviously, the integration region Φ in (26) brings the constraint

$$|\delta_k| \le \zeta, \forall k = 1,2,\cdots,K, \tag{91}$$

such that all the $\zeta-|\delta_k|$ must be positive. Hence, with the constraint

$$\mathbf{1}_K^{\mathrm{T}}\boldsymbol{\delta} = \sqrt{K}h, \tag{92}$$

the maximum of $\prod_{k=1}^{K}(\zeta-|\delta_k|)$ must occur in the region $\delta^+ = \{\delta_k > 0, \forall k = 1,2,\cdots,K\}$, because given any $\boldsymbol{\delta}$ containing negative elements, there always exists a certain $\boldsymbol{\delta}$ in the region δ^+ leading to a larger $\prod_{k=1}^{K}(\zeta-|\delta_k|)$. Thus, we have

$$\sum_{k=1}^{K}\zeta-|\delta_k| = \sum_{k=1}^{K}\zeta-\delta_k = K\zeta-\sqrt{K}h, \tag{93}$$

which is a positive constant. Based on the arithmetic-geometric mean inequality, the maximum of $\prod_{k=1}^{K}(\zeta-|\delta_k|)$ occurs if and only if $\delta_k = \frac{h}{\sqrt{K}}$, $\forall k = 1,2,\cdots,K$, and thus Property 1 is proved. ■

Accordingly, the first term in (89) becomes

$$\max_{\boldsymbol{\delta}:\mathbf{1}_K^{\mathrm{T}}\boldsymbol{\delta}=\sqrt{K}h} P_{\mathrm{L}}\frac{\prod_{k=1}^{K}(\zeta-|\delta_k|)}{\zeta^K} = P_{\mathrm{L}}\left(1-\frac{h}{\sqrt{K}\zeta}\right)^K. \tag{94}$$

The maximum of the second term occurs at [37][5]

$$\boldsymbol{\delta} = \sqrt{K}h\frac{\boldsymbol{J}^{-1}\mathbf{1}_K}{\mathbf{1}_K^{\mathrm{T}}\boldsymbol{J}^{-1}\mathbf{1}_K}, \tag{95}$$

such that it becomes

$$\max_{\boldsymbol{\delta}\in\Delta:\mathbf{1}_K^{\mathrm{T}}\boldsymbol{\delta}=\sqrt{K}h} P_{\mathrm{S}}(\boldsymbol{\delta}) = \mathcal{Q}\left(\frac{\sqrt{K}h}{2\sqrt{\mathbf{1}_K^{\mathrm{T}}\boldsymbol{J}^{-1}\mathbf{1}_K}}\right). \tag{96}$$

Correspondingly, (89) is further written as

$$\begin{aligned} &\max_{\boldsymbol{\delta}:\mathbf{1}_K^{\mathrm{T}}\boldsymbol{\delta}=\sqrt{K}h} P(\boldsymbol{\delta})\frac{\prod_{k=1}^{K}(\zeta-|\delta_k|)}{\zeta^K} \\ &\approx P_{\mathrm{L}}\left(1-\frac{h}{\sqrt{K}\zeta}\right)^K + \begin{cases} \mathcal{Q}\left(\frac{\sqrt{K}h}{2\sqrt{\mathbf{1}^{\mathrm{T}}\boldsymbol{J}^{-1}\mathbf{1}}}\right)-P_{\mathrm{L}} & 0\le h\le\tilde{h}, \\ 0 & h>\tilde{h}, \end{cases} \end{aligned} \tag{97}$$

where $\tilde{h}$ is the threshold derived via (87), i.e.,

$$\frac{\sqrt{K}\tilde{h}}{2\sqrt{\mathbf{1}_K^{\mathrm{T}}\boldsymbol{J}^{-1}\mathbf{1}_K}} \approx \sqrt{2T\left[\left(\frac{M\eta_1\|\boldsymbol{\beta}\|_2^2}{2+M\eta_1\|\boldsymbol{\beta}\|_2^2}\right)^2 + \sum_{k=L+1}^{K}\left(\frac{M\eta_k}{2+M\eta_k}\right)^2\right]} \tag{98}$$

with the constraint $0 \le \tilde{h} \le \sqrt{K}\zeta$.

[5] Since the array observation data are related to the wanted random parameters (i.e., DOAs) and other unwanted random parameters (e.g., sources and noise power), we cannot simply calculate $\boldsymbol{J}^{-1}$ only considering the Fisher information w.r.t. $\boldsymbol{\theta}$ [1, Chap. 8]. In this case, the parameter vector containing all random parameters is $\boldsymbol{\alpha} = [\boldsymbol{\theta}^{\mathrm{T}}, \boldsymbol{\sigma}^{\mathrm{T}}]^{\mathrm{T}}$ with $\boldsymbol{\sigma} = [\sigma_1^2, \sigma_2^2, \cdots, \sigma_K^2, \sigma_n^2]^{\mathrm{T}}$ denoting the unwanted parameter vector, and the complete Fisher information matrix $\boldsymbol{J}_{\boldsymbol{\alpha}}$ can be calculated according to (9) or (54) by replacing $\boldsymbol{\theta}$ into $\boldsymbol{\alpha}$. Then, $\boldsymbol{J}^{-1}$ should be calculated as the first block with $K\times K$ elements in $\boldsymbol{J}_{\boldsymbol{\alpha}}^{-1}$, whose explicit solution is given in [17, Eq. (3.1)] for overdetermined DOA estimation and [19, Eq. (43)] for underdetermined DOA estimation, respectively.

Then, (14) can be further written as

$$\begin{aligned}\frac{1}{K}\mathbf{1}_K^{\mathrm{T}}\boldsymbol{R}_{\boldsymbol{\epsilon}}\mathbf{1}_K \geq P_{\mathrm{L}}&\int_0^{\sqrt{K}\zeta}\left(1-\frac{h}{\sqrt{K}\zeta}\right)^K hdh\\ &+\int_0^{\tilde{h}}\left[\mathcal{Q}\left(\frac{\sqrt{K}h}{2\sqrt{\mathbf{1}_K^{\mathrm{T}}\boldsymbol{J}^{-1}\mathbf{1}_K}}\right)-P_{\mathrm{L}}\right]hdh,\end{aligned} \tag{99}$$

where the first integration

$$\int_0^{\sqrt{K}\zeta}\left(1-\frac{h}{\sqrt{K}\zeta}\right)^K hdh = \frac{12\mathrm{Tr}\{\boldsymbol{R}_{\boldsymbol{\theta}}\}}{(K+1)(K+2)}, \tag{100}$$

and the second integration

$$\begin{aligned}&\int_0^{\tilde{h}}\left[\mathcal{Q}\left(\frac{\sqrt{K}h}{2\sqrt{\mathbf{1}_K^{\mathrm{T}}\boldsymbol{J}^{-1}\mathbf{1}_K}}\right)-P_{\mathrm{L}}\right]hdh\\ &=\int_0^{\tilde{h}}\frac{1}{\sqrt{2\pi}}e^{-\frac{Kh^2}{8\mathbf{1}_K^{\mathrm{T}}\boldsymbol{J}^{-1}\mathbf{1}_K}}\frac{\sqrt{K}h^2}{4\sqrt{\mathbf{1}_K^{\mathrm{T}}\boldsymbol{J}^{-1}\mathbf{1}_K}}dh\\ &=\Gamma_{\frac{3}{2}}(\tilde{u})\frac{\mathbf{1}_K^{\mathrm{T}}\boldsymbol{J}^{-1}\mathbf{1}_K}{K}.\end{aligned} \tag{101}$$

with $\tilde{u}$ defined in (30).

References

[1] H. L. Van Trees, *Detection, Estimation, and Modulation Theory, Part IV: Optimum Array Processing*. Wiley, 2002.

[2] R. O. Schmidt, "Multiple emitter location and signal parameter estimation," *IEEE Trans. Antennas Propag.*, vol. 34, no. 3, pp. 276–280, Mar. 1986.

[3] B. D. Rao and K. V. S. Hari, "Performance analysis of root-MUSIC," *IEEE Trans. Acoust., Speech, Signal Process.*, vol. 37, no. 12, pp. 1939–1949, Dec. 1989.

[4] C.-L. Liu and P. P. Vaidyanathan, "Remarks on the spatial smoothing step in coarray MUSIC," *IEEE Signal Process. Lett.*, vol. 22, no. 9, pp. 1438–1442, Sep. 2015.

[5] R. Roy and T. Kailath, "ESPRIT-estimation of signal parameters via rotational invariance techniques," *IEEE Trans. Acoust., Speech, Signal Process.*, vol. 37, no. 7, pp. 984–995, Jul. 1989.

[6] F.-M. Han and X.-D. Zhang, "An ESPRIT-like algorithm for coherent DOA estimation," *IEEE Antennas and Wireless Propag. Lett.*, vol. 4, pp. 443–446, Dec. 2005.

[7] F.-J. Chen, S. Kwong, and C.-W. Kok, "ESPRIT-like two-dimensional DOA estimation for coherent signals," *IEEE Trans. Aerosp. Electron. Syst.*, vol. 46, no. 3, pp. 1477–1484, July 2010.

[8] D. Malioutov, M. Çetin, and A. S. Willsky, "A sparse signal reconstruction perspective for source localization with sensor arrays," *IEEE Trans. Signal Process.*, vol. 53, no. 8, pp. 3010–3022, Aug. 2005.

[9] C. Zhou, Y. Gu, X. Fan, Z. Shi, G. Mao, and Y. D. Zhang, "Direction-of-arrival estimation for coprime array via virtual array interpolation," *IEEE Trans. Signal Process.*, vol. 66, no. 22, pp. 5956–5971, Nov. 2018.

[10] C. Zhou, Y. Gu, Z. Shi, and Y. D. Zhang, "Off-grid direction-of-arrival estimation using coprime array interpolation," *IEEE Signal Process. Lett.*, vol. 25, no. 11, pp. 1710–1714, Sep. 2018.

[11] A. M. Elbir, "DeepMUSIC: Multiple signal classification via deep learning," *IEEE Sens. Lett.*, vol. 4, no. 4, pp. 1–4, Apr. 2020.

[12] A. Barthelme and W. Utschick, "A machine learning approach to DoA estimation and model order selection for antenna arrays with subarray sampling," *IEEE Trans. Signal Process.*, vol. 69, pp. 3075–3087, May 2021.

[13] G. K. Papageorgiou, M. Sellathurai, and Y. C. Eldar, "Deep networks for direction-of-arrival estimation in low snr," *IEEE Trans. Signal Process.*, vol. 69, pp. 3714–3729, Jun. 2021.

[14] H. L. Van Trees and K. L. Bell, *Bayesian Bounds for Parameter Estimation and Nonlinear Filtering/Tracking*. New York, NY, USA: Wiley, 2007.

[15] H. Cramér, *Mathematical Methods of Statistics*. Princeton University Press, 1946.

[16] P. Stoica and A. Nehorai, "MUSIC, maximum likelihood and Cramér-Rao bound," *IEEE Trans. Acoust., Speech, Signal Process.*, vol. 37, no. 5, pp. 720–741, May 1989.

[17] ——, "Performance study of conditional and unconditional direction-of-arrival estimation," *IEEE Trans. Acoust. Speech Signal Process.*, vol. 38, no. 10, pp. 1783–1795, Oct. 1990.

[18] M. Wang and A. Nehorai, "Coarrays, MUSIC, and the Cramér-Rao bound," *IEEE Trans. Signal Process.*, vol. 65, no. 4, pp. 933–946, Feb. 2017.

[19] C.-L. Liu and P. Vaidyanathan, "Cramér-Rao bounds for coprime and other sparse arrays, which find more sources than sensors," *Digit. Signal Process.*, vol. 61, pp. 43–61, Feb. 2017.

[20] A. Renaux, P. Forster, P. Larzabal, C. D. Richmond, and A. Nehorai, "A fresh look at the Bayesian bounds of the Weiss-Weinstein family," *IEEE Trans. Signal Process.*, vol. 56, no. 11, pp. 5334–5352, Jun. 2008.

[21] A. Weiss and E. Weinstein, "A lower bound on the mean-square error in random parameter estimation," *IEEE Trans. Inf. Theory*, vol. 31, no. 5, pp. 680–682, Sep. 1985.

[22] I. Reuven and H. Messer, "A Barankin-type lower bound on the estimation error of a hybrid parameter vector," *IEEE Trans. Info. Theory*, vol. 43, no. 3, pp. 1084–1093, 1997.

[23] A. Renaux, P. Forster, P. Larzabal, and C. Richmond, "The Bayesian Abel bound on the mean square error," in *Proc. IEEE Int. Conf. Acoust. Speech Signal Process.*, vol. 3, Toulouse, France, May 2006, pp. III–III.

[24] B. Bobrovsky and M. Zakai, "A lower bound on the estimation error for certain diffusion processes," *IEEE Trans. Info. Theory*, vol. 22, no. 1, pp. 45–52, Jan. 1976.

[25] J. Ziv and M. Zakai, "Some lower bounds on signal parameter estimation," *IEEE Trans. Inf. Theory*, vol. 15, no. 3, pp. 386–391, May 1969.

[26] L. Seidman, "Performance limitations and error calculations for parameter estimation," *Proc. IEEE*, vol. 58, no. 5, pp. 644–652, May 1970.

[27] D. Chazan, M. Zakai, and J. Ziv, "Improved lower bounds on signal parameter estimation," *IEEE Trans. Inf. Theory*, vol. 21, no. 1, pp. 90–93, Jan. 1975.

[28] X. Gu and M. Wong, "A modified Ziv-Zakai lower bound and its application in array processing," in *Proc. Int. Conf. Acoust. Speech Signal Process.*, vol. 2, Apr. 1991, pp. 1477–1480.

[29] B. M. Sadler, N. Liu, and Z. Xu, "Ziv-Zakai bounds on time delay estimation in unknown convolutive random channels," *IEEE Trans. Signal Process.*, vol. 58, no. 5, pp. 2729–2745, May 2010.

[30] D. Khan and K. L. Bell, "Explicit Ziv-Zakai bound for analysis of DOA estimation performance of sparse linear arrays," *Signal Process.*, vol. 93, no. 12, pp. 3449–3458, Dec. 2013.

[31] N. Decarli and D. Dardari, "Ziv-Zakai bound for time delay estimation of unknown deterministic signals," in *Proc. IEEE Int. Conf. Acoust., Speech Signal Process.*, Florence, Italy, May 2014, pp. 4673–4677.

[32] V. M. Chiriac, Q. He, A. M. Haimovich, and R. S. Blum, "Ziv-Zakai bound for joint parameter estimation in MIMO radar systems," *IEEE Trans. Signal Process.*, vol. 63, no. 18, pp. 4956–4968, Jun. 2015.

[33] K. V. Mishra and Y. C. Eldar, "Performance of time delay estimation in a cognitive radar," in *Proc. IEEE Int. Conf. Acoust., Speech Signal Process.*, New Orleans, LA, Mar. 2017, pp. 3141–3145.

[34] T. Laas and W. Xu, "On the Ziv-Zakai bound for time difference of arrival estimation in CP-OFDM systems," in *Proc. IEEE Wireless Commun. Networking Conf. (WCNC)*, Nanjing, China, Mar. 2021, pp. 1–5.

[35] Z. Zhang, Z. Shi, C. Zhou, C. Yan, and Y. Gu, "Ziv-Zakai bound for compressive time delay estimation," *IEEE Trans. Signal Process.*, pp. 1–13, June 2022.

[36] K. L. Bell, Y. Steinberg, Y. Ephraim, and H. L. Van Trees, "Extended Ziv-Zakai lower bound for vector parameter estimation," *IEEE Trans. Inf. Theory*, vol. 43, no. 2, pp. 624–637, Mar. 1997.

[37] K. L. Bell, Y. Ephraim, and H. L. Van Trees, "Explicit Ziv-Zakai lower bound for bearing estimation," *IEEE Trans. Signal Process.*, vol. 44, no. 11, pp. 2810–2824, Nov. 1996.

[38] Z. Yang, P. Stoica, and J. Tang, "Source resolvability of spatial-smoothing-based subspace methods: A hadamard product perspective," *IEEE Trans. Signal Process.*, vol. 67, no. 10, pp. 2543–2553, May 2019.

[39] Z. Zheng, Y. Huang, W.-Q. Wang, and H. C. So, "Direction-of-arrival estimation of coherent signals via coprime array interpolation," *IEEE Signal Process. Lett.*, vol. 27, pp. 585–589, Mar. 2020.

[40] H. Zheng, C. Zhou, Z. Shi, and Y. Gu, "Structured tensor reconstruction for coherent DOA estimation," *IEEE Signal Process. Lett.*, vol. 29, pp. 1634–1638, July 2022.

[41] H. L. Van Trees, *Detection, Estimation, and Modulation Theory, Part III: Radar-Sonar Signal Processing and Gaussian Signal in Noise*. Wiley, 2001.

[42] S. M. Kay, *Fundamentals of Statistical Signal Processing, Volume I: Estimation Theory*. Prentice Hall PTR, 1993.
[43] G. Casella and R. Berger, *Statistical Inference*. Thomson Learning, 2002.
[44] P. Pal and P. P. Vaidyanathan, "Coprime sampling and the MUSIC algorithm," in *Proc. IEEE Digit. Signal Process. Workshop / IEEE Singal Process. Education Workshop (DSP/SPE)*, Sedona, AZ, Jan. 2011, pp. 289–294.
[45] Z. Zhang, C. Zhou, Y. Gu, J. Zhou, and Z. Shi, "An IDFT approach for coprime array direction-of-arrival estimation," *Digit. Signal Process.*, vol. 94, pp. 45–55, Nov. 2019.